energies

MDPI

Review

Surface Passivation to Improve the Performance of Perovskite Solar Cells

Hayeon Lee [1] and Dawen Li [2,*]

[1] Department of Chemical and Biological Engineering, The University of Alabama, Tuscaloosa, AL 35487, USA; hlee110@crimson.ua.edu
[2] Department of Electrical and Computer Engineering, The University of Alabama, Tuscaloosa, AL 35487, USA
* Correspondence: dawenl@eng.ua.edu

Abstract: Perovskite solar cells (PSCs) suffer from a quick efficiency drop after fabrication, partly due to surface defects, and efficiency can be further enhanced with the passivation of surface defects. Herein, surface passivation is reviewed as a method to improve both the stability and efficiency of PSCs, with an emphasis on the chemical mechanism of surface passivation. Various molecules are utilized as surface passivants, such as halides, Lewis acids and bases, amines (some result in low-dimensional perovskite), and polymers. Multifunctional molecules are a promising group of passivants, as they are capable of passivating multiple defects with various functional groups. This review categorizes these passivants, in addition to considering the potential and limitations of each type of passivant. Additionally, surface passivants for Sn-based PSCs are discussed since this group of PSCs has poor photovoltaic performance compared to their lead-based counterpart due to their severe surface defects. Lastly, future perspectives on the usage of surface passivation as a method to improve the photovoltaic performance of PSCs are addressed to provide a direction for upcoming research and practical applications.

Keywords: perovskite solar cells; efficiency and stability; passivation mechanisms; surface defects; Sn-based perovskite

Citation: Lee, H.; Li, D. Surface Passivation to Improve the Performance of Perovskite Solar Cells. *Energies* **2024**, *17*, 5282. https://doi.org/10.3390/en17215282

Academic Editor: Lin Mao

Received: 12 August 2024
Revised: 16 September 2024
Accepted: 15 October 2024
Published: 24 October 2024

1. Introduction

Organic-inorganic perovskite has the chemical formula of ABX_3, where A is a large cation (MA^+ (methylammonium) or FA^+ (formamidinium)) or a small cation of Cs^+, B is the central metal ion (Pb^{2+} or Sn^{2+}), and X is a halogen ion (Br^-, Cl^-, or I^-). It consists of a $BX_6{}^{4-}$ octahedral cube with A cations between the cubes [1]. Organic-inorganic perovskite is usually chosen due to its low-cost solution processing and the feasibility of tuning the bandgap; however, it has the critical disadvantage of sensitivity to ambient environments and degradation [2]. A perfect crystalline structure is not always achieved, and imperfect lattices with defects such as vacancies, interstitials, antisites, interrupted lattices at the surface, or grain boundaries with undercoordinated ions and dangling bonds exist, as shown in Figure 1 [3]. Defects such as undercoordinated halogen ions, lead ions, Pb-I antisites, iodine, methylammonium (MA^+), and formamidinium (FA^+) vacancies exist at the grain boundaries. Due to these defects, the surface and grain boundaries are susceptible to external factors such as light, heat, water, oxygen, etc. [4]. These defects trap charged carriers, which reduces the charged carrier lifetime and diffusion length [5]. Consequently, defects act as the primary sites for non-radiative recombination, which is the leading cause of reduced fill factors (FFs) and an open-circuit voltage (V_{OC}) [6]. In other words, surface defects on perovskite film reduce the efficiency and stability of PSCs. Therefore, many methods are utilized to combat the effects of an imperfect lattice, such as surface passivation [7–9], an additive to the perovskite precursor solution or antisolvent [10,11], and interface engineering [12,13]. Because defects on the film surface are the leading cause of reduced stability and efficiency, surface passivation is one of many solutions available to

increase the power conversion efficiency (PCE) and durability of PSCs. A vast variety of materials are used for surface passivation, such as small molecules and polymers. Although this review only focuses on perovskite-based solar cells, surface passivation strategies have also been applied to other emerging thin-film solar cell technologies, such as organic solar cells [14,15].

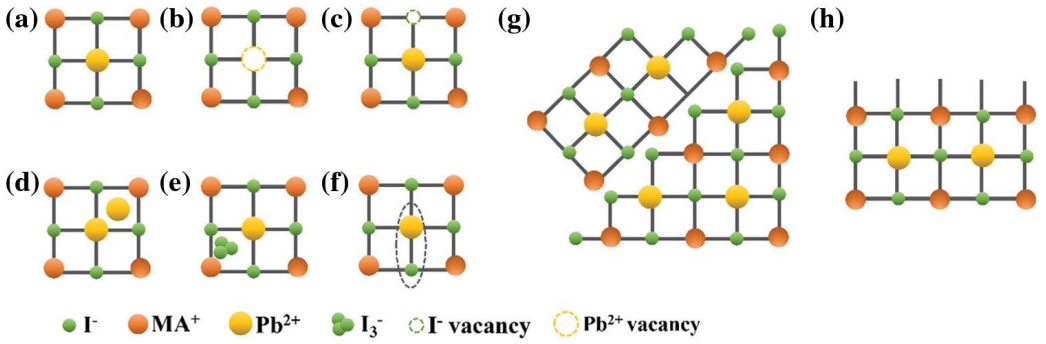

Figure 1. Illustration of surface defects in PSCs [3]. Diagram (**a**) shows a lattice without any defects. Diagrams (**b**,**c**) demonstrate Pb^{2+} and I^{-} vacancies, respectively; diagrams (**d**,**e**) illustrate interstitial Pb^{2+} and I^{3-} ions, respectively. Diagram (**f**) illustrates the antisite substitution of Pb–I. Lastly, diagrams (**g**,**h**) show the grain boundary of perovskite crystals and dangling bonds on the surface of perovskite, respectively.

To thoroughly delve into the role of surface passivants of PSCs, this review will investigate common categories of surface passivants: materials that form low-dimensional perovskites, small molecules (halides, Lewis acids and bases, amines, and multifunctional molecules), and polymers. Each of these materials utilizes a differing chemical mechanism to passivate the surface defects of perovskite films, which will be explored in detail in their respective sections. Examples of PSCs with these passivants are provided in each section, along with the fundamentals and limitations of each type of passivant. In addition, this review explores the surface passivants of Sn-based PSCs, as Sn-based perovskites contain more surface defects as compared to their lead-based counterparts. However, they are eco-friendly and widely used in tandem solar cells. By examining the surface passivants of PSCs from a chemical standpoint, the extensive review seeks to inform readers about the possibilities of surface passivation as a method of improving the photovoltaic performance of PSCs.

2. Materials That Result in Low-Dimensional Perovskite

Low-dimensional (LD) perovskites are used due to their beneficial effects on the stability and efficiency of PSCs. LD perovskites are divided into 0D, 1D, and 2D structures according to their size and shape [16]. For applications in PSCs, 1D and 2D perovskites are often utilized. One-dimensional structures are depicted by nanorods and nanowires, while 2D structures are represented by nanoplatelets and flat layered structures [17,18]. Because of the differences in the size and dimension of these LD materials, as shown in Figure 2, a quantum size effect is present [19]. In other words, LD perovskites have differing electron energy levels and bandgaps compared to their 3D counterparts. Researchers use these vastly different properties of LD perovskites as a method of surface passivation for perovskite film. For instance, LD perovskites have fewer dangling bonds and more exposed AX layers than 3D perovskite crystals [20]. This leads to the enhanced stability of the resulting device. Furthermore, it is common for LD layers to act as a buffer layer to prevent humidity-induced degradation of the 3D perovskite layer [21]. However, a common problem in LD perovskite films is that the transportation of the charged carriers is inhibited by molecules forming the LD perovskite due to their long alkyl chains. Additionally, LD perovskite has a larger bandgap, and the mobility of its charged carriers has decreased compared to that of its 3D counterpart [22]. Therefore, it is essential to choose a suitable

LD perovskite-forming molecule to gain the benefits of the LD layer while avoiding the negative effects.

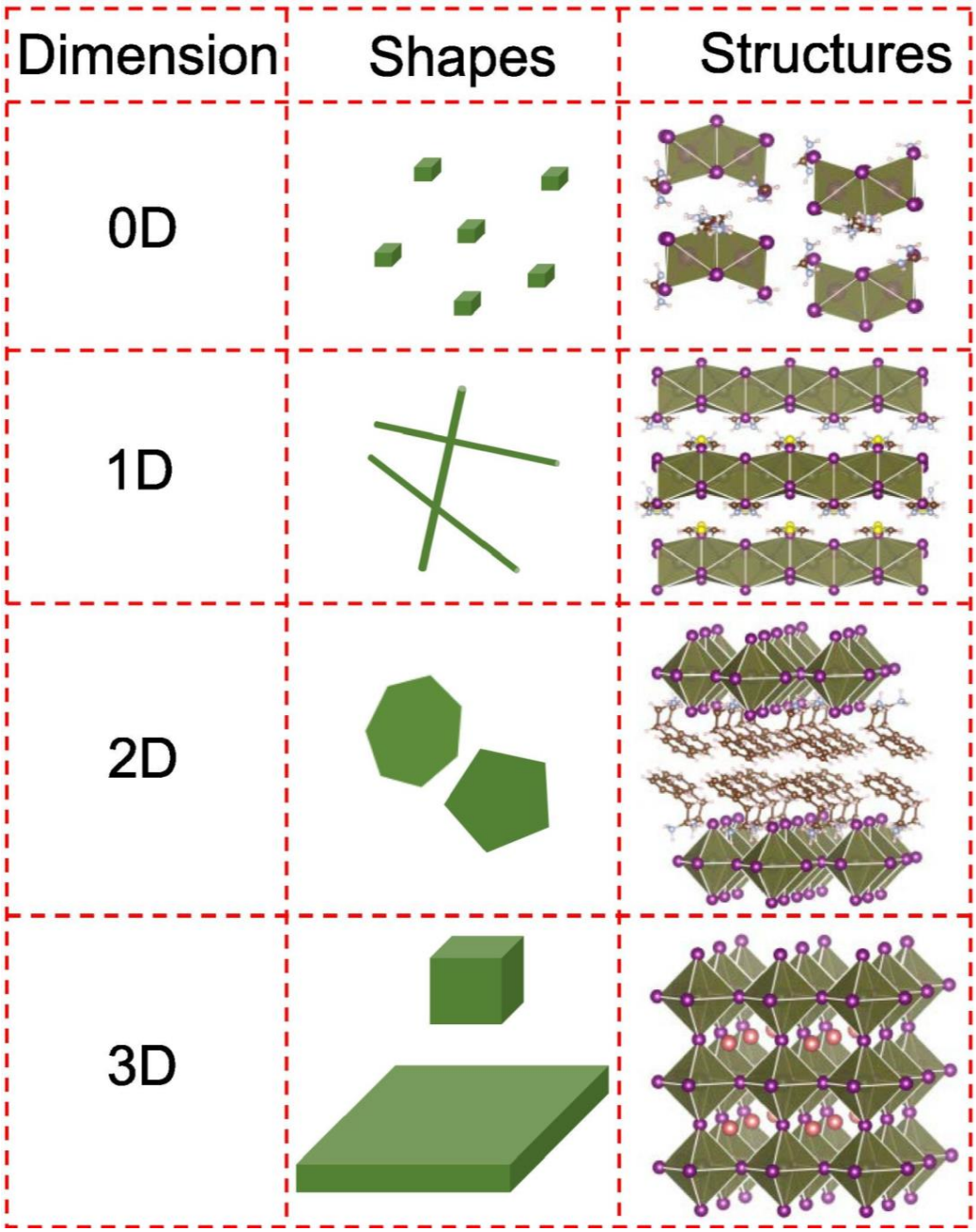

Figure 2. The chart showcases the shapes and the chemical structures of the LD perovskites [19]. 1D perovskites are represented as nanorods. Two-dimensional perovskites are displayed as a flat layer or nanoplatelets. Lastly, 3D perovskites are shown as a solid material with their three dimensions in length, width, and height.

2.1. One-Dimensional Perovskite

The 1D/3D heterostructure of the perovskite layer is utilized for the advantageous effect of the 1D perovskite, acting as a barrier to prevent humidity and heat from degrading the 3D perovskite layer [23]. Consequently, the stability of the perovskite film is enhanced when 1D perovskite is formed on the 3D perovskite [24]. Moreover, the 1D perovskite layer can passivate defects on the surface and grain boundaries of the 3D perovskite crystals, which enhances the overall photovoltaic performance of the resulting PSC.

To utilize the benefits of a 1D perovskite layer, Zhou et al. applied 2-amidinopyridine hydrochloride (2AP) as a surface passivant to form a 1D/3D heterostructured perovskite layer [25]. The nitrogen atom in pyridine allows the ring to have a strong Lewis acid-base reaction with positively charged defects such as undercoordinated Pb^{2+} ions. 2AP has a relatively large moment of dipole, which results in a significant interaction between the perovskite and 2AP. The addition of 2AP to the perovskite results in a homogenous layer of 1D perovskite on the 3D perovskite. This 1D perovskite passivates grain boundary defects, enhances the humidity stability of the resulting device by causing the film to be more hydrophobic than before the 2AP treatment, and improves the interface with the hole transport layer (HTL) due to the smooth surface morphology. The resulting device, with a structure of glass/ITO/SnO_2/PbI_2FAMA/2AP/Spiro-OMeTAD/Au, demonstrated a PCE of 24.55% with enhanced stability in high-humidity environments.

Although many of the effects of 1D/3D heterostructured perovskite are advantageous, as seen above, some disadvantages are caused by the LD perovskite layer. For example, the formation of 1D perovskites could interfere with charge carrier transport. As a result, some groups have discovered ways to reduce the negative effects while utilizing the benefits of the LD perovskite layer. For instance, Cha et al. utilized pyridinium bromide (PyBr) to form a 1D/3D perovskite heterostructure [26]. The IPA-dissolved PyBr was spin-coated on FAMA $PbI_{3-x}Br_x$ perovskite film, which formed pyridinium-based 1D perovskite, as shown in Figure 3. This is due to the difference in the size of the ions of the perovskite (FA^+ and MA^+) and the pyridinium ion. Because the pyridinium ion is larger in size compared to FA^+ and MA^+ ions, 1D perovskite is formed. This newly formed LD perovskite layer matches the lattice of the 3D perovskite, which leads to the enhanced alignment of the energy band. Additionally, the pyridinium ion does not interfere with the extraction and transportation of charged carriers because it is relatively small. The resulting device, with a structure of glass/ITO/SnO_2/PbI_3PbBr_3FAMA/PyBr/Spiro-OMeTAD/Au, had a PCE of 23.74% with enhanced humidity tolerance. In short, this group carefully chose their surface passivant to form 1D perovskites and prevent the LD layer from interfering with the movement of charge carriers.

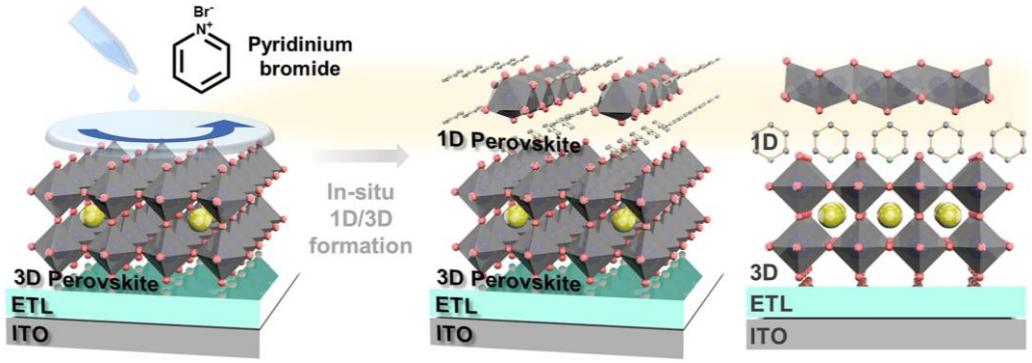

Figure 3. The illustration showcases the process and the chemical structure of the 1D/3D heterostructure formed by pyridinium bromide [26]. PyBr is spin-coated on the 3D perovskite on top of the SnO_2 electron transport layer (ETL) and ITO. This leads to the formation of 1D perovskite on the 3D perovskite layer, which is shown above.

In a similar fashion, Gu et al. used benzamidine hydrochloride (BHCl) to form a modified 1D perovskite layer on the FAMA$PbI_{3-x}Cl_x$ perovskite film [27]. As mentioned above, a common problem that LD perovskite films have is that the transportation of charged carriers is inhibited by the fully covered LD perovskite on the 3D perovskite film. Accordingly, BHCl was spin-coated on the FAMA$PbI_{3-x}Cl_x$ perovskite film to form a 1D perovskite layer with a similar structure to a net. The addition of the BHCl passivated the surface defects of 3D perovskite without fully covering the film to enhance the charge transport. Similarly, when growing an LD perovskite layer across all the film, the BHCl-

induced, discontinuous 1D perovskite layer improved the hydrophobicity of the film. The resulting device, with a structure of glass/FTO/SnO_2/PbI_2PbCl_2FAMA/BHCl/Spiro-OMeTAD/Au, had a PCE of 24.6%. Instead of relying on the size of the ions from the surface passivant to prevent interference with the charged carrier movement, this group discovered a way to form a discontinued, net-like, structured LD layer to make the most of the benefits of the LD layer while avoiding the negative side effects.

In short, the formation of 1D perovskites on the 3D perovskite absorber layer, introducing a surface passivant, is a promising technique to improve the efficiency and stability of PSCs. However, the 1D/3D heterostructured perovskite layer has adverse effects, such as the reduced extraction and transportation of charged carriers. If researchers can discover a way to lessen these effects, such as forming a net-like structured 1D perovskite layer or utilizing a surface passivant with ions that are relatively small to avoid interference with the charged carrier transport, the benefits of the 1D perovskite layer can be employed to their fullest potential.

2.2. Two-Dimensional Perovskite

The 2D/3D heterostructure of perovskite film is utilized due to its advantageous effects of 2D perovskite acting as a layer to block the 3D perovskite from humidity and oxygen, decrease the migration of ions, increase the hydrophobic qualities of the film, and increase the formation energy [28]. The heterostructure introduces new energy levels to increase the charge extraction and transport. As stated in the previous section, there are many defects on the surface and grain boundary of the film [29]. As a result, any measure to renovate the surface defects improves the quality of the perovskite film, which increases the efficiency and stability of the overall PSCs.

Many groups have investigated the usage of octyl ammonium iodide (OAI) as a passivant of PSCs. For example, Jeong et al. used OAI as a passivant and formed a 2D/3D heterostructured perovskite in PSCs with a structure of glass/FTO/c-TiO_2/m-TiO_2/Fo-$FAPbI_3$ (FAHCOO added perovskite)/OAI/Spiro-OMeTAD/Au [30]. The ammonium salt passivated the FA^+ vacancies and reduced the non-radiative recombination caused by excess lead iodide. Furthermore, the $FAPbI_3$ perovskite film was doped with pseudo-halide anion formate ($HCOO^-$) to reduce the vacancy of anions at the surface and grain boundaries of the film. The resulting device had a certified PCE of 25.2% and more normalized PCEs when exposed to 20% relative humidity and 65 °C for 1000 h than the untreated device. Although OAI resulted in PSCs with high PCEs in the aforementioned group, Wang et al. found a differing result. In contrast to the previous studies, this study found a decrease in PCE when glass/FTO/SnO_2/$CsFAMAPbI_3$/OAI/Spiro-OMeTAD/Au-structured PSCs were treated with OAI [31]. The authors theorize that although OAI passivates undercoordinated vacancies at the surface of $CsFAMAPbI_3$ perovskite film, the long alkyl chain of OAI causes an increase in carrier transport resistance. There was a reduction in PCE from 18.63% in the control devices to 17.72% in the OAI-treated devices. A significant decrease in the average open-circuit voltage (V_{OC}) and fill factor (FF) of OAI-treated devices was also observed, which is seen in Figure 4.

However, this does not rule out the possibility that OAI is an effective passivant of PSCs, as Choi et al. discovered a way to utilize the benefits of OAI without the adverse effects of the long alkyl chain of OAI [32]. Choi et al. deposited aluminum oxide (AlO) on OAI-treated PSCs with a structure of glass/FTO/c-TiO_2/mp-TiO_2/$FAPbI_3$/OAI/AlO/Spiro-OMeTAD/Au to exploit the benefits of OAI as a passivant without the negative side effects. The aluminum ions from AlO diffused into the perovskite, which led to the consistent transportation of charged carriers. Light-induced 2D perovskite was also formed, which reduced the degradation of PSCs induced by light. The resulting device had a PCE of 23.75% and maintained a normalized PCE of 95% when exposed to 1 SUN continuous illumination for 1000 h, as seen in Figure 5. In short, OAI is a beneficial surface passivant of PSCs if the adverse effects of the long alkyl chain increasing the carrier transport resistance can be hindered.

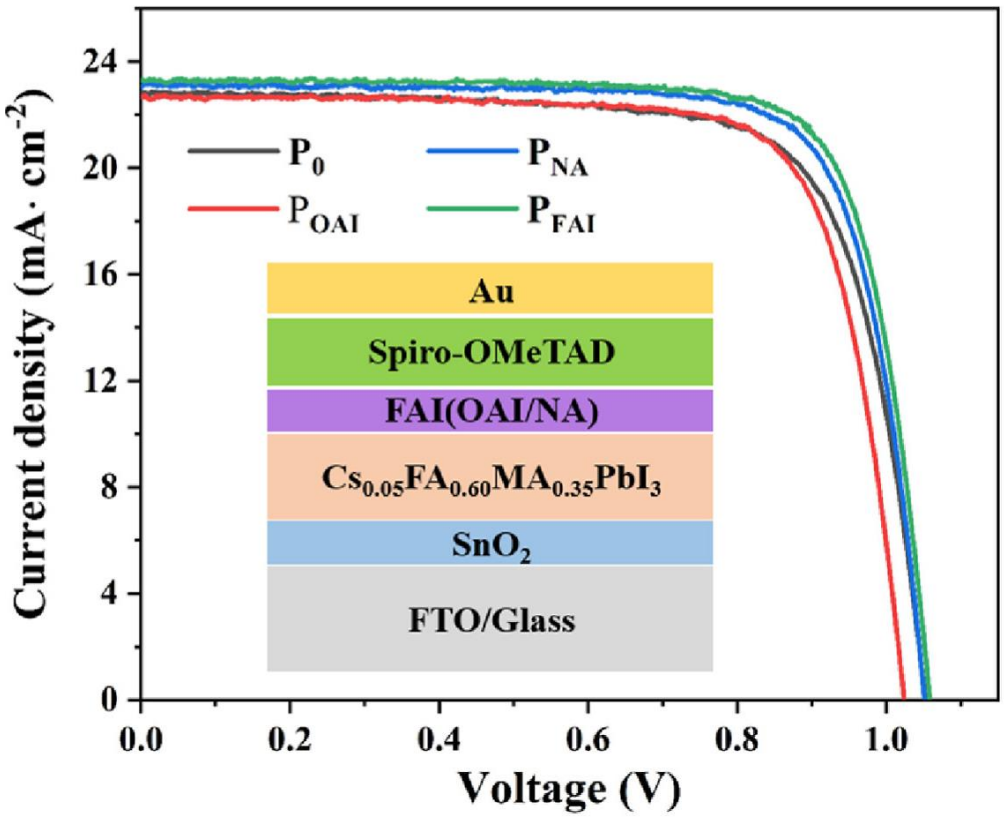

Figure 4. The figure above displays the decrease in short-circuit current density (J_{SC}) and open-circuit voltage (V_{OC}) when devices were treated with OAI [31]. The J_{SC} decreased from 22.84 mA·cm^{-2} of the control sample to 22.68 mA·cm^{-2} of the sample with OAI treatment. The V_{OC} also reduced from 1.05 V of the control sample to 1.03 V of the OAI sample. Additionally, the diagram within the J-V curve shows the structure of the device: glass/FTO/SnO_2/$CsFAMAPbI_3$/OAI/Spiro-OMeTAD/Au.

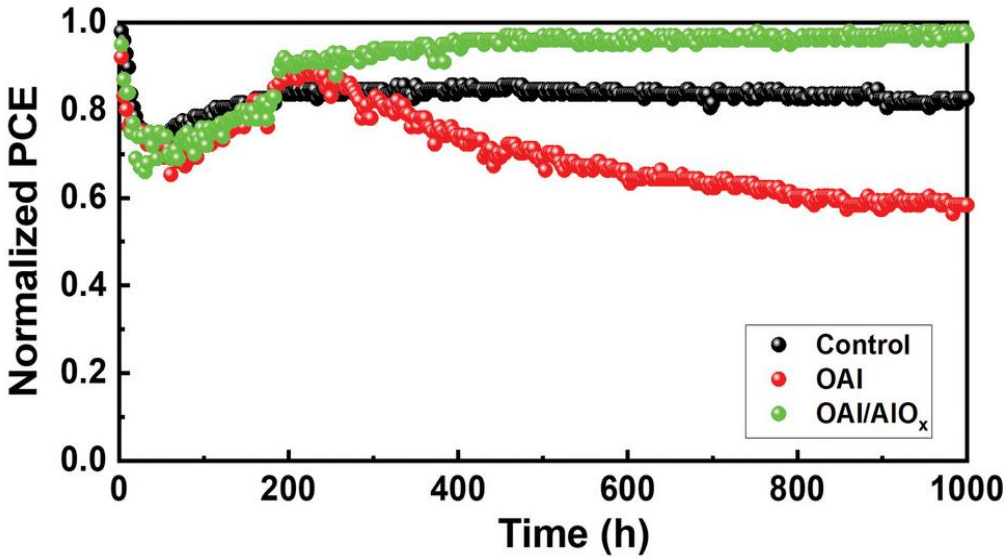

Figure 5. Graph D demonstrates how the normalized PCE of PSC treated with OAI and AlO was higher than those of the control and PSC with only OAI when exposed to 1 SUN continuous illumination for 1000 h in ambient conditions [32].

Other molecules than OAI are used by many researchers to create a 2D/3D heterostructured perovskite layer. For example, Luo et al. utilized hexylammonium bromide (HABr) dissolved in Cl_2-dissolved chloroform to passivate the 3D perovskite absorber layer and form a 2D/3D heterostructure on the 3D perovskite layer [33]. The dissolved Cl_2 interacted with the 3D perovskite, which led to an ionic exchange of chlorine and iodine and additional bulk grain growth. The resulting chlorine ions passivated the defects at the grain boundaries of the perovskite layer. Moreover, HABr formed a 2D/3D heterostructure on the surface of the perovskite absorber, which led to a high-quality perovskite film with reduced surface defects and an increase in the size of the grains. HABr-treated PSCs with a structure of glass/ITO/SnO_2/CsFAMAPbI$_{3-x}$Br$_x$/HABr with Cl_2-CF/Spiro-OMeTAD/Ag had a PCE of 24.21% with significantly higher stability than the control device.

Similarly, Yoo et al. utilized n-hexylammonium bromide (n-HABr) as a passivant of the perovskite ($FAMAPbI_3$ with a trace amount of $MAPbBr_3$) film of PSCs with a structure of glass/FTO/SnO_2/KCl/$FAMAPbI_3$ with $MAPbBr_3$/n-HABr/Spiro-OMeTAD/Au [34]. The alkylammonium bromide formed a 2D perovskite layer on the 3D perovskite film, which resulted in a longer carrier lifetime compared to the control. The trace amount of $MAPbBr_3$ added to the perovskite led to the diffusion of Br^- ions in the perovskite film, with MACl being slowed, which resulted in a growth in the size of the grains and the lifetime of the charge carriers. Additionally, this group tuned the deposition of SnO_2 to create an optimized ETL and passivated the interface between the SnO_2 ETL and perovskite film with KCl, which will be further explored in Section 3.1. The resulting device had a certified PCE of 25.2%. It can be seen that the 2D perovskite layer enhances the size of the perovskite crystals, which leads to an improvement in the lifetime of charged carriers. This method has great potential to further improve the photovoltaic performance of PSCs, as the results are promising, with a PCE of over 24%.

Additionally, 2D perovskite layers can also improve the alignment of energy bands between the perovskite layer and the HTL. For example, Tan et al. investigated the usage of long-chain dodecylammonium halides (DACl, DABr, and DAI) as surface passivants of $CsFAMAPbI_3$-based PSCs [35]. All three of these halides can form 2D/3D heterostructures, but the layer formed by DACl was the most effective at passivating surface defects, increasing the extraction and transportation of charged carriers, and enhancing the alignment of the energy band between the HTL and the perovskite layer. The result from X-ray photoelectron spectroscopy confirmed that DACl interacted with undercoordinated Pb^{2+} ions, and the results from X-ray diffraction proved that the DA_2PbCl_4 2D perovskite layer formed once the perovskite layer was treated with DACl. As shown in Table 1, the DACl-treated device with a structure of glass/ITO/SnO_2/$CsFAMAPbI_3$/DA_2PbCl_4/Spiro-OMeTAD/Ag resulted in a PCE of 23.91% and a normalized PCE of 95% after 1000 h of humidity aging at room temperature.

Table 1. Lists of different passivators used to passivate the $CsFAMAPbI_3$ perovskite layer and the resulting J_{SC}, V_{OC}, FF, and PCE [35]. The J_{SC} increased from 24.69 mA·cm^{-2} of the control sample to 24.80 mA·cm^{-2} of the sample with DACl treatment. The V_{OC} also improved from 1.132 V of the control sample to 1.174 V of the DACl sample. Moreover, the fill factor increased from 81.01% of the control to 82.11% of the DACl sample. Lastly, the PCE followed the same trend as the J_{SC}, V_{OC}, and FF, as the control PCE was 22.66% and the DACl-treated PCE was 23.91%.

PSCs	J_{SC} [mA cm^{-2}]	V_{OC} [V]	FF [%]	PCE [%]
Control	24.69	1.132	81.01	22.66
DACl	24.80	1.174	82.11	23.91
DABr	24.97	1.165	81.76	23.78
DAI	24.79	1.163	81.29	23.45

Similarly, Li et al. used 4,4-difluoropiperidine hydrochloride (2FPD) on 3D $CsFAMAPbI_3$ perovskite to form a 2D perovskite layer [36]. The resulting $(2FPD)_2PbI_4$ or 2D perovskite improved the energy-level alignment at the interface between the 3D perovskite layer

and HTL, enhancing the transport of charged carriers. Furthermore, it passivated surface defects on the perovskite layer by donating a lone pair of electrons to undercoordinated Pb^{2+} ions and forming hydrogen bonds with the iodine of the perovskite. The resulting device, with a structure of glass/FTO/MeO-4PACz/$CsFAMAPbI_3$/2FPD/PCBM/BCP/Cu, had a certified PCE of 24.38% with improved humidity and thermal stability compared to the control, as shown in Figure 6. In other words, not only does the 2D perovskite layer improve the crystallinity of the resulting perovskite film, reducing the defects, but it also improves the energy band alignment between the perovskite layer and the HTL to further enhance charge transport, improving both the efficiency and stability of the PSC.

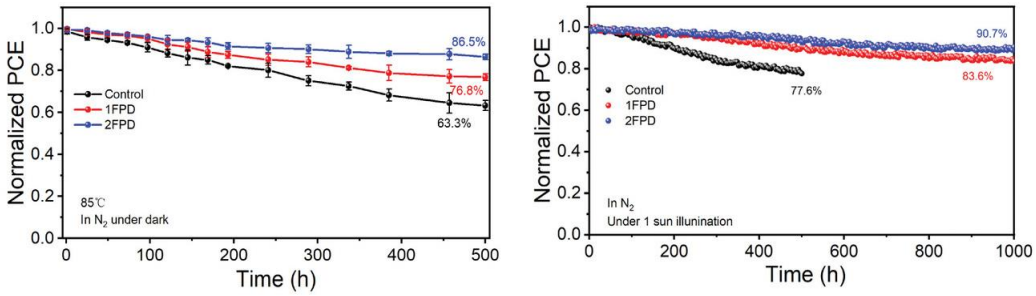

(**a**) (**b**)

Figure 6. The graphs above illustrate the improved normalized PCEs of 2FPD-modified PSCs [36]. Graph (**a**) demonstrates how PSC with 2FPD had a normalized PCE of 86.5% after being exposed to 85 °C for 500 h in N_2 in the dark compared to the control, which had a normalized PCE of 63.3% under the same conditions. Graph (**b**) shows how 2FPD-modified PSC had a higher normalized PCE of 90.7% compared to that of the control devices, at 77.6%, when exposed to 1 SUN illumination in N_2 for 1000 h.

Some researchers opted to use a combination of different molecules to form 2D perovskite crystals. The first molecule passivates the surface defects; then, the second molecule passivates defects at the grain boundary. For instance, Gong et al. employed both 2-thiazolamide hydrochloride (SFACl) and methylamine sulfate (MA_2SO_4) as passivants for a Cs–Pb–mixed perovskite layer [37]. The addition of SFACl to the perovskite layer formed a 2D/3D heterostructure: SFA_2PbI_4 and $CsPbI_3$. This is due to the significant polar properties of SFACl and the interaction between the sulfur from SFACl and the undercoordinated Pb^{2+} ion from the perovskite layer, which increases the size of the perovskite grains. As shown in Figure 7, MA_2SO_4 was added to the film after SFACl was spin-coated on the perovskite layer, which induced the formation of $PbSO_4$. This resulted in the passivation of defects at the grain boundaries, which caused the charged carrier lifetime to increase. The resulting device, with a structure of glass/ITO/PTAA/PEAI-$CsFAMAPbI_{3-x}Br_x$/SFACl/MA_2SO_4/PCBM-C_{60}/$Zr(acac)_4$/Au, had a certified PCE of 23.02%. As described above, using two different molecules not only passivated the surface defects on the 3D perovskite film but also passivated the dangling bonds at the grain boundary of the 2D perovskite layer.

In short, a 2D/3D heterostructured perovskite layer is used by many researchers as it improves the alignment of energy bands, enhances the crystallinity of the film, and passivates defects at the surface and grain boundaries of the film. Although some materials have been found to have adverse effects when used as a surface passivant to form the 2D perovskite layer, if optimized accordingly, the materials that form 2D perovskite crystals have promising uses in future endeavors.

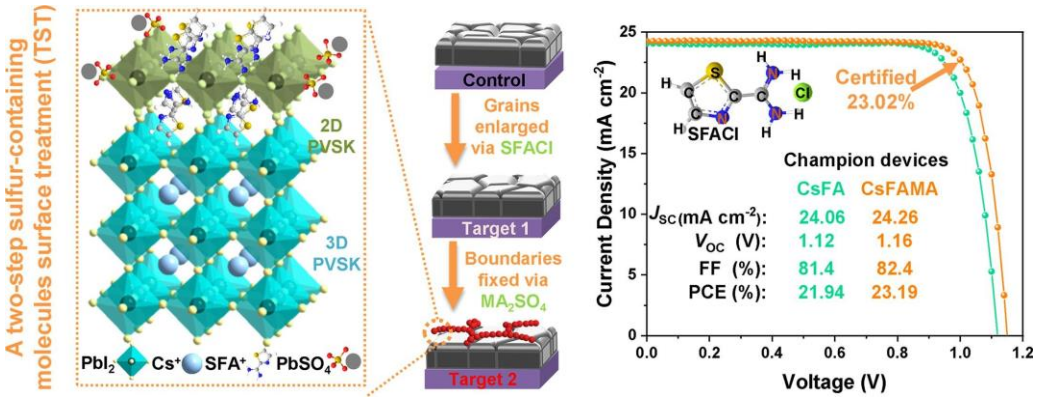

Figure 7. The diagram above illustrates the structure of the 2D/3D heterostructure of perovskite when passivated with SFACl and MA_2SO_4 [37]. SFACl causes growth in the grain sizes of the perovskite, while the MA_2SO_4 passivates defects on the grain boundary. The resulting PCEs of the device with these passivants are listed in the graph on the right: 21.94% with CsFA, 23.19% with CsFAMA.

3. Small Molecules

3.1. Halides

Undercoordinated halide anions are one of the main defects on the surface of perovskite films [38]. These defects can trap positively charged holes, resulting in non-radiative recombination and a reduced photovoltaic performance [39]. Halogen bonds (XB) can passivate these defects and enhance the structural order of the perovskite, which results in an increase in the efficiency and stability of PSCs.

It is common for halides, such as those with chloride and bromide ions, to take advantage of their ability to passivate iodine vacancies and undercoordinated Pb^{2+} ions as surface passivants of perovskite films. For example, Shao et al. utilized bis(2-chloroethyl)ammonium chloride (B(CE)ACl) as a surface passivant between the FAMA PbI_3 perovskite film and the Spiro-OMeTAD HTL [40]. The symmetric geometry of the $B(CE)A^+$ cation assisted in the passivation of undercoordinated Pb^{2+} ions on the perovskite film, as the symmetrical geometry results in a stronger dipole moment at the terminals of the halide compared to asymmetric 2-chloroethylammonium cation (CEA^+). The dipole moment was created by the halogen anion, Cl^-, and the ammonium group, which is positively charged. Therefore, there was a better alignment of the energy band between the perovskite film and the HTL, an enhanced extraction of holes, and reduced t non-radiative recombinations. The resulting device, with a structure of glass/FTO/SnO_2/FAMAPbI_3/B(CE)ACl/Spiro-OMeTAD/Au, had a PCE of 25.6% and enhanced stability compared to the control.

Similarly, Chen et al. utilized 1-methyl-3-benzyl-imidazolium bromide (BzMIMBr) as a surface passivant of $FAPbI_3$ perovskite film [41]. The Br^- ions and nitrogen atoms from BzMIMBr passivated iodine vacancies and undercoordinated Pb^{2+} ions, respectively, on the surface of the perovskite film. An interesting finding from this study is that not only did the BzMIMBr passivate surface defects, but it also passivated defects at the grain boundaries in the bulk perovskite. The resulting device, with a structure of glass/FTO/SnO_2/$FAPbI_3$/BzMIMBr/Spiro-OMeTAD/Au, had a PCE of 25.3% with better stability than the control device.

Additionally, Liu et al. utilized Cs_3MnBr_5:Ce^{3+} nanocrystals and 1H,1H-perfluorooctylamine iodide (PFOAI) as surface passivants of PSCs [42]. The nanocrystal was utilized to passivate the interface between the SnO_2 ETL and the perovskite layer, and the PFOAI was used to passivate the interface between the perovskite layer and the Spiro-OMeTAD HTL. The nanocrystal enhanced the surface morphology of the SnO_2 layer, which reduced the likelihood of FTO coming into contact with the perovskite layer. However, PFOAI is hydrophobic due to the use of functional groups with fluorine, which enhances the humidity stability of the resulting device. Additionally, the incorporation of the halide salt resulted in the passivation of iodine vacancies on the surface of the per-

ovskite film and an enhancement in the alignment of the energy level for the improved extraction and transportation of charged carriers. The resulting device, with a structure of glass/FTO/SnO_2/Cs_3MnBr_5:Ce^{3+}/CsFAMAPbI_3PbBr_3/PFOAI/Spiro-OMeTAD/Ag, had a PCE of 24.24%. It can be seen from the previous examples that utilizing halides on Pb-based perovskite films when Spiro-OMeTAD is used as the HTL is significantly effective at improving the photovoltaic performance of the resulting PSCs. This can be attributed to the ability of these halides to act as surface passivants to form halogen bonds and enhance the structural integrity of the perovskite crystals.

On the other hand, some researchers utilized halides to passivate the interface between the ETL and perovskite layer. For example, as stated in Section 2.2, Yoo et al. utilized KCl as a surface passivant of the interface between the SnO_2 ETL and PbI_2FAMA perovskite film [34]. In addition to the n-HABr forming a 2D perovskite layer on the perovskite film, KCl reacted with undercoordinated Sn^{4+} ions and passivated oxygen vacancies that were prominent on the surface of the SnO_2 layer. This resulted in a much more stabilized ETL with reduced defects at the ETL and perovskite layer interface, which led to the increased extraction and transportation of electrons. The resulting PSCs, with a structure of glass/FTO/SnO_2/KCl/PbI_2FAMA with $MAPbBr_3$/n-HABr/Spiro-OMeTAD/Au, had a certified PCE of 25.2%. In other words, not only are halides a beneficial passivant of the interface between the HTL and the perovskite layer, but they also have advantageous effects as a surface passivant of the interface between the SnO_2 ETL and the Pb-based perovskite layer. Because one of the main issues with SnO_2 ETL is the degradation resulting from oxidation's reaction with the perovskite layer, KCl, and other halide salts are materials with great potential for improving the efficiency and stability of PSCs with metal oxide charge transport layers.

3.2. Lewis Acids and Bases

Lewis acids and bases are used for their interaction with surface defects. For example, Lewis acids can accept electron pairs and form acid–base complexes without transferring electrons through covalent bonding. This suggests their potential to passivate negatively charged defects, such as PbI^{3-} antisites and I^- excess [2]. On the other hand, Lewis bases can donate electron pairs and passivate positively charged defects, such as undercoordinated positively charged Pb^{2+} ions and lead interstitials [43–45]. Likewise, zwitterions possess the traits of both Lewis acids and Lewis bases, which can passivate both positively charged and negatively charged surface defects [46].

Lewis bases are a common surface passivant at the interface between the Pb–Cs–mixed perovskite layer and HTL, used to passivate undercoordinated Pb^{2+} ions. For example, Cheng et al. engineered tetraethyl [(2,7-dibromo-9H-fluorene-9,9-diyl)di(ethane-2,1-diyl)]bis(phosphonate) (DPPO) as a surface passivant of CsFAMA-based perovskite film [47]. This molecule was specifically made for its two phosphonate groups, which interacted with undercoordinated positively charged lead ions due to its significantly high polar characteristics. In other words, DPPO acted as a Lewis base to passivate undercoordinated Pb^{2+} ions. Furthermore, DPPO improved the energy level alignment, which increased the extraction of charged carriers and reduced non-radiative recombination. The resulting device, with a structure of glass/ITO/SnO_2/CsFAMAPbI_3PbBr_3/DPPO/PEAI/Spiro-OMeTAD/MoO/Ag, had a PCE of 24.42% with increased environmental stability.

Similar usage of Lewis base can be seen when 4-aminophenyl sulfone (APS) was utilized as a surface passivant of $CsFAMAPbI_3$ perovskite film [48]. This molecule is a Lewis base, as the oxygen atom that double-bonds to the sulfur atom donates its lone pair of electrons to undercoordinated Pb^{2+} ions on the surface of the perovskite layer. This resulted in a reduction in non-radiative recombination on the surface of the film, thereby improving its stability. Furthermore, the addition of APS established a buffer layer between the perovskite film and Spiro-OMeTAD HTL, which improved the hydrophobicity of the film. The resulting device, with a structure of glass/ITO/SnO_2/$CsFAMAPbI_3$/APS/Spiro-OMeTAD/Ag, had a PCE of 23.03% with enhanced thermal stability and humidity tolerance.

As shown above, when used as a surface passivant of the interface between the Cs-Pb-based perovskite layer and Spiro-OMeTAD HTL, engineered Lewis bases are materials with significant potential to enhance the photovoltaic performance of PSCs as they can passivate positively charged defects.

On the other hand, some groups utilized Lewis bases to passivate the interface between the HTL and perovskite layer in an inverted PSC structure. For example, Yuan et al. utilized 4-pyrazolecarboxylic acid (4-PCA) as a surface passivant of the interface between NiOx HTL and the perovskite layer [49]. When 4-PCA was introduced to the interface, a Lewis acid–base interaction was formed between the nitrogen atom in 4-PCA and the undercoordinated Pb^{2+} ions, as shown in Figure 8. This led to the passivation of surface defects on the perovskite film, as well as an enhancement of the extraction of holes. Moreover, 4-PCA acted as a buffer layer at the interface to prevent the redox reaction between the NiOx and perovskite that forms trap densities to promote non-radiative recombination. In other words, 4-PCA enhanced the crystal quality of the perovskite and reduced sites of non-radiative recombination. The resulting device, with a structure of glass/ITO/NiOx/4-PCA/CsFAMAPbI$_{3-x}$Br$_x$/BzMIMBr/PCBM/BCP/Ag, had a PCE of 23.77%, with enhanced humidity and thermal stability. Not only are Lewis bases an effective surface passivant of the interface between the perovskite layer and the HTL in a regular PSC structure, but they can also be utilized at the interface between metal oxide HTL and the perovskite layer in an inverted PSC structure. The redox reaction between metal oxide HTL and the perovskite layer is one of the main issues with using beneficial metal oxides as the HTL. As a result, Lewis bases are a promising material in the future of PSCs, allowing for the usage of metal oxide transport layers while avoiding adverse effects.

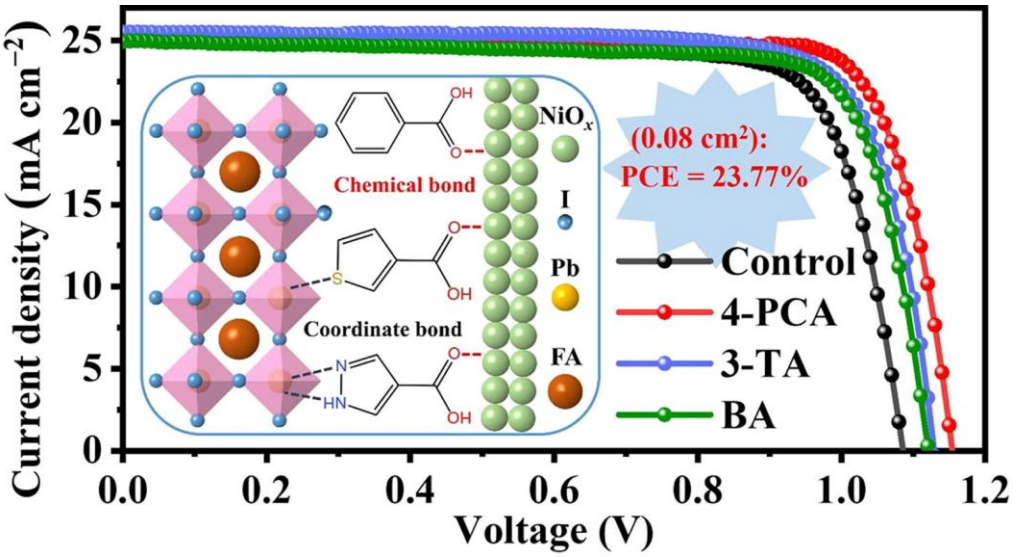

Figure 8. The diagram above illustrates how BA, 3-TA, and 4-PCA, respectively, interact with the perovskite and NiOx layers [49]. The pink structure on the left is the perovskite layer, and the green structure on the right is the NiOx HTL. The molecule on the bottom, 4-PCA, forms a Lewis acid-base interaction with the perovskite. The graph displays the J-V curve of the following devices: control, 4-PCA-treated, 3-TA-treated, and BA-treated. It can be observed that the device with 4-PCA treatment had a higher J_{OC} and V_{OC} than the control device.

Although Lewis bases are effective surface passivants, their most significant limitation is that they can only passivate positively charged defects. On the other hand, zwitterions share traits with both Lewis acids and Lewis bases, which makes them desirable surface passivant, as they can passivate both positively and negatively charged defects on the surface of the perovskite film. For example, Wang et al. utilized L-tryptophan (Trp), an amino acid, to passivate the interface between the perovskite film and NiOx HTL [50]. Trp is a zwitterion, a molecule with both cationic and anionic groups, which can passivate both positively

charged and negatively charged surface defects. As shown in Figure 9, the anionic carboxyl group, –COO–, passivated oxygen vacancies on the NiOx HTL, and the cationic ammonium group, $–NH_3^+$, interacted with undercoordinated iodine and bromine ions on the surface of the perovskite film and filled in the vacancies of FA^+, MA^+, and Pb^{2+}. In addition to passivating the surface defects, Trp also acted as a buffer layer to prevent defect-inducing redox reactions from occurring, which enhanced the long-term stability of the PSC. The resulting device, with a structure of glass/ITO/NiOx/Trp/$CsFAMAPbI_{3-x}Br_x$/C_{60}/BCP/Ag, had a PCE of 23.79%.

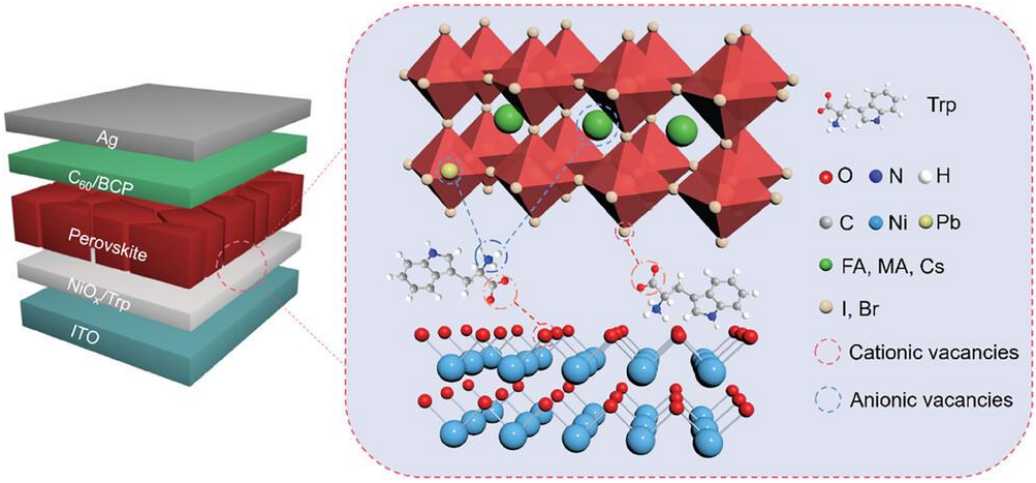

Figure 9. The diagram above illustrates the structure of PSC with the Trp interface between NiOx and the perovskite layer: ITO/NiO/Trp/Perovskite/C_{60}/BCP/Ag [50]. The interaction between Trp and NiO HTL and the perovskite layer is shown on the right, where Trp passivates both cationic and anionic vacancies.

Similarly, Yu et al. investigated the usage of 1-amino pyridine iodine (AmPyl) as a surface passivant of PSCs [51]. Instead of a traditional Lewis acid or base, AmPyl is a zwitterion, which can passivate both positively charged and negatively charged defects concurrently. AmPyl passivated defects at the surface and grain boundary of perovskite by forming hydrogen bonds. In addition, iodine ions from AmPyl passivated undercoordinated lead ions. This led to improved grain growth and elongated the lifetime of the charged carriers. As a result, the device with the structure of glass/ITO/SnO_2/$CsFAMAPbI_{3-x}Br_x$/AmPyl/Spiro-OMeTAD/Ag had a PCE of 23.80%. As seen in these results, the ability of zwitterions to passivate both cationic and anionic defects is significantly advantageous compared to Lewis bases or acids, which are only able to passivate positively charged or negatively charged defects, respectively.

3.3. Amines

Unlike some amines that are utilized to induce the formation of low-dimensional perovskite layers, the amines categorized in this section are used to passivate surface defects without forming low-dimensional and 3D perovskite heterostructures. Amines have multiple advantages as a surface passivant of PSCs [52]. For example, linear amines promote the enhanced growth of crystals to improve the quality of perovskite films [53]. Additionally, aromatic amines are used as passivants due to the hydrophobic quality of the benzene ring [54,55].

Although certain amines have the possibility of forming a low-dimensional perovskite layer, in some cases, forming a surface passivant layer is more effective at suppressing defects and enhancing the photovoltaic performance of the resulting device than forming an LD/3D heterostructured perovskite layer. For example, Jiang et al. investigated the usage of phenyl ammonium iodide (PEAI) as a surface passivant on $FAMAPbI_3$ perovskite film [56]. PEA^+ or the cations from PEAI could form a 2D layer on the surface of the perovskite lattice.

However, here, the authors demonstrated that the PEAI serves as a surface passivant of the $FAMAPbI_3$ perovskite layer instead of forming a 2D PEA_2PbI_4 perovskite layer. The results from monitoring photoluminescence intensities and X-ray crystallography have shown that the use of a PEAI layer to suppress surface defects results in reduced non-radiative recombination and increases the charged carrier lifetime without forming a 2D PEA_2PbI_4 layer. The PEAI layer passivated the iodine vacancy, as seen in the results from Pb 4*f* and I 3*d* core-level energy spectra. Furthermore, the PEAI passivation led to the slowing of perovskite film degeneration. The resulting glass/ITO/SnO_2/PbI_3FAMA/PEAI/Spiro-OMeTAD/Au-structured PSC had a certified PCE of 23.32%.

Similarly, a mixture of two different amines with differing dipole moments and ion sizes can be utilized to prevent the formation of the LD layer. Although the presence of the LD perovskite layer is beneficial in certain cases, it is not always advantageous to have an LD/3D heterostructure for the perovskite layer. As a result, Ma et al. utilized both phenylmethylammonium iodide (PMAI) and OAI as surface passivants of the $FAMAPbI_3$ perovskite layer [57]. The mixture of PMAI and OAI, interestingly, did not result in the formation of a 2D/3D heterostructure but resulted in a thin layer of the ammonium halide forming on the perovskite layer. Because OA^+ is equipped with a stronger stable dipole moment than PMA^+, OA^+ was more quickly absorbed into the perovskite film than PMA^+. This inhibited the PMA^+ from forming a 2D perovskite layer and prevented the reduction in charged carrier extraction due to the presence of a 2D perovskite layer. Moreover, the results from time-resolved photoluminescence (TRPL) showed that the average lifetime of a charged carrier was significantly longer for devices with both PMAI and OAI treatment compared to the use of only one of the passivants. The resulting device, with a structure of glass/FTO/SnO_2/PbI_3FAMA/PMAI and OAI/Spiro-OMeTAD/Au, had a certified PCE of 25.0%.

Likewise, the same group utilized two amines with the high formation energy required to form a 2D perovskite layer to take advantage of the ability of these amines to improve the efficiency and stability of PSCs. Shi et al. investigated the usage of carbazole-9-ethylammonium iodide (CzEAI) and 3,6-dimethyl-carbazole-9-ethylammonium iodide (MeEAI) as surface passivants of PSCs [58]. Because CzEAI and MeEAI have molecular pi-pi interactions and higher steric hindrance when attaching to the surface of the perovskite layer, the formation energy required to form a 2D perovskite layer is higher than linear PEAI. This prevents the formation of a 2D/3D heterostructure of perovskite at room temperature and at high temperatures of up to 85 °C. In addition to preventing the formation of 2D, the density of surface defects was decreased, which led to the MeEAI-treated device with the structure of glass/ITO/SnO_2/$CsFAMAPbI_2$/MeEAI/Spiro-OMeTAD/MoO/Ag achieving a PCE of 25.1% and maintaining a normalized PCE of 90% when operated with maximum power point tracking for 400 h. In short, many ways of using amines as a surface passivant of Pb-based perovskite layers while avoiding the formation of LD perovskite crystals have been studied by researchers when it is not beneficial to have the heterostructure of LD on 3D perovskites.

Not only is it essential to consider the combination of amines used to prevent the LD perovskite layer, but the length and size of the amine used must also be considered. Wang et al. investigated the usage of propane-1,3,-diamine dihydroiodide ($PDAI_2$), methyl enediamine dihydroiodide ($MDAI_2$), and pentane-1,5-diamine dihydroiodide ($PentDAI_2$) as surface passivants of a CsFAMA-based perovskite film [59]. These three molecules were selected to determine the optimum molecular size of the passivant, and it was found that $PDAI_2$ had the most effective chain length for the passivation of perovskite film. The $PDAI_2$ treatment led to a reduction in iodine vacancies, which led to the better extraction of electrons compared to the control. The glass/ITO/MeO-2PACz/$RbCsFAMAPbI_{3-x}Br_x$/$PDAI_2$/C_{60}/BCP/Ag-structured device had a PCE of 25.81% and improved operational stability. In other words, it is significantly important to examine and optimize the size of the molecule used as a surface passivant to maximize the enhancement of the photovoltaic performance of resulting PSCs.

If all of the conditions mentioned above are optimized, the effects of the use of amines as a surface passivant of the interfaces above and below the perovskite layer, or the ETL and HTL, are significant. For example, Wu et al. utilized PMI, or a mixture of PEAI and methylammonium iodide (MAI), to passivate the interface between PTAA HTL and the perovskite layer and the interface between the perovskite layer and C_{60} ETL [53]. The addition of PMI at the interface between HTL and the perovskite layer improved the crystallinity of perovskite, as well as the wettability of the perovskite precursor solution on the HTL. Additionally, the presence of PMI at the interface between perovskite and ETL led to the passivation of FA^+-, Pb^{2+}-, and I^- affiliated defects, which reduces non-radiative recombination. The resulting device, with a structure of glass/FTO/PTAA/PMI $FAMAPbI_3$/PMI/C_{60}/BCP/Ag, had a PCE of 24.20%, with enhanced thermal and humidity stability compared to the control, which is shown in Figure 10.

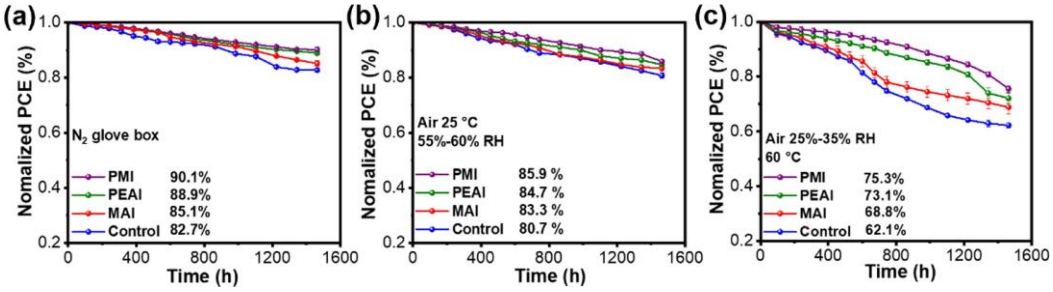

Figure 10. Graphs (**a**–**c**) illustrate the enhanced stabilities of PMI-modified PSCs when exposed to various conditions for 1600 h: N_2 atmosphere for graph A, 55% to 60% relative humidity in ambient air at room temperature for graph B, and 60 °C for graph C [53].

Additionally, Yang et al. utilized guanidinium phosphate (GP) as a bidirectional passivant of $FAMAPbI_3$ perovskite film [60]. Instead of only passivating the surface of the perovskite film, GP passivated both the surface defects of the perovskite film and those of the neighboring SnO_2 ETL. This resulted in further improvements in the stability and efficiency of the resulting PSCs as it enabled the alignment of energy levels between these layers and prevented the migration of ions. The phosphate ion of GP bonded with Sn^{4+} on the SnO_2 ETL, which resulted in a high-quality film. In addition, the amino group of GP formed hydrogen bonds with iodine ions of the perovskite absorber layer, which passivated surface defects and improved the quality of the film. The resulting device, with a structure of glass/ITO/GP-SnO_2/$FAMAPbI_3$/Spiro-OMeTAD/Ag, had a PCE of 23.91% with improved humidity stability and an improved fill factor. In short, the amino group of amines often forms hydrogen bonds with iodine ions of the perovskite layer, which improves the surface quality of the film, in addition to other benefits that are unique to each of the amines. Even when amines do not form an LD perovskite layer, they are still molecules with promising properties as a surface passivant of PSCs if optimized accordingly.

3.4. Multifunctional Molecules

On the other hand, molecules with multiple functional groups have stronger passivating effects compared to molecules with single functional groups. Multifunctional molecules can passivate multiple defects on the surface of the perovskite film, which enhances the stability and efficiency of perovskite solar cells [61–68]. Many multifunctional molecules form hydrogen bonds with the perovskite surface, which reduces ion migration, leading to an increase in the stability and efficiency of the PSC [69,70].

For example, Zhu et al. investigated the usage of 4-tert-butyl-benzylammonium iodide (tBBAI) as a surface passivant for perovskite film [71]. The treatment increased the extraction of charge carriers from the perovskite layer to the hole-transport layer and decreased the non-radiative recombination. The resulting tBBAI-treated PSC, with a

structure of glass/FTO/c-TiO_2/m-TiO_2/CsFAMA$PbI_{3-x}Br_x$/tBBAI/Spiro-OMeTAD/Au, reached a PCE of 23.5%, which is higher than the PCE of the control device, at 20%. Furthermore, the tert-butyl group of tBBAI provided hydrophobic qualities to the surface of the perovskite film, which increased its stability. Consequently, it retained over 90% of its original PCE after exposure to ambient air with a relative humidity of 50–70%. When tBBAI-treated PSC was exposed to 500 h of full sun illumination under maximum-powerpoint tracking, it had a normalized PCE of over 95%.

Additionally, the amino group, carbonyl group, and chloride ion are beneficial functional groups, as they passivate undercoordinated Pb^{2+} ions and form hydrogen bonds with the perovskite layer. Wu et al. utilized 2-amino-5-chlorobenzophenone (ACB) as a surface passivant of FAMA $PbI_{3-x}Br_x$ perovskite film [72]. The carbonyl and nitrogen of the amino groups of ACB passivated undercoordinated positively charged Pb^{2+} ions on the surface of the perovskite film. Both the amino and chloride groups formed hydrogen bonds with the perovskite, which limited the deterioration of the film. The resulting device, with a structure of glass/FTO/TiO_2/FAMA$PbI_{3-x}Br_x$/ACB/Spiro-OMeTAD/Au, had a PCE of 24.32% with improved ambient stability when stored for 1440 h in ambient conditions. As shown above, specific functional groups, in this case, amino, chloride, and carbonyl groups, are utilized for their beneficial effects as surface passivants of FAMA$PbI_{3-x}Br_x$-based PSCs.

Other combinations of functional groups are used as well, such as aldehyde, hydroxyl, and alkoxy groups, to passivate the interface between FAMA $PbI_{3-x}Br_x$ perovskite absorber and Spiro-OMeTAD HTL. Lu et al. used 3-ethoxy-4-hydroxybenzadehyde (EVL) as a surface passivant of FAMA$PbI_{3-x}Br_x$ perovskite film [73]. Different functional groups of EVL inhibited defects, which reduced non-radiative recombination and enhanced the movement of holes from perovskite to the hole transport layer. For example, the aldehyde of EVL passivated undercoordinated, positively charged Pb^{2+} ions. Moreover, the hydroxyl and alkoxy groups formed hydrogen bonds at the interface of the perovskite film to prevent ion migration, especially the migration of formamidine ions and iodide ions. This repressed ion migration led to a reduction in hysteresis as well. The resulting device, with a structure of glass/FTO/TiO_2/FAMA$PbI_{3-x}Br_x$/EVL/Spiro-OMeTAD/Au, had a PCE of 24.1% with improved stability.

Similarly, Zhang et al. utilized an organic potassium salt, KCFSO, as a multi-functional surface passivant of $FAPbI_3$ perovskite [74]. Unlike inorganic potassium salts that require significant polar solvents, KCFSO is very soluble in isopropanol. Furthermore, KCFSO has multiple functional groups, such as fluorine atoms that form hydrogen bonds with undercoordinated FA^+ ions, an $–SO_3^-$ group that forms a Lewis acid-base interaction with undercoordinated Pb^{2+} ions, and a double bond between sulfur and oxygen atoms that passivates positively charged defects such as undercoordinated Pb^{2+} ions and iodine vacancies. KCFSO treatment resulted in defect passivation, a reduction in trap densities compared to the control, and the enhanced transportation of charged carriers. The resulting device, with a structure of glass/FTO/SnO_2/$FAPbI_3$/KCFSO/Spiro-OMeTAD/Au, had a PCE of 25.11%. In this case, a potassium salt with fluorine atoms, a sulfur oxide group, and a double bond passivated the surface of the $FAPbI_3$ perovskite film by forming hydrogen bonds with undercoordinated FA^+ ions, forming Lewis acid-base interactions with undercoordinated Pb^{2+} ions, and passivating undercoordinated Pb^{2+} ions and iodine vacancies. This combination of functional groups was clearly beneficial to the performance of the resulting device, as the resulting PCE was over 25%.

On the other hand, instead of passivating the interface between the perovskite layer and HTL, some groups focused on the interface between the ETL and perovskite layer. For example, Bian et al. utilized 5-[4-[1,2,2-tri[4-(3,5-dicarboxyphenyl)phenyl]ethylene]phenyl]benzene-1,3-dicarboxylic acid (H_8ETTB) as an interface passivant between SnO_2 ETL and the perovskite layer [75]. H_8ETTB has multiple functional groups, such as a carboxyl group, aromatic ether, benzene rings, biphenyl groups, and conjugated double bonds, that are valuable for the interface. For example, the carboxyl group of H_8ETTB interacted with undercoordinated Sn^{2+} and oxygen vacancies, resulting in an improvement in the adjustment of energy

levels. This led to the significantly better transportation of charged carriers compared to the control. In addition, H_8ETTB passivated undercoordinated Pb^{2+} ions on the surface of the perovskite film, which improved the crystallinity of perovskite. Most importantly, H_8ETTB enhanced the stability of the resulting device by converting degradation-inducing UV light into perovskite-absorbable light. As a result, the H_8ETTB-modified device with the structure of glass/FTO/SnO_2/H_8ETTB/CsFAMAPb$I_{3-x}Br_x$/Spiro-OMeTAD/Ag had a PCE of 23.32%. In short, multifunctional molecules are versatile, as it is feasible to optimize their usage as a surface passivant of interfaces other than the one between the perovskite layer and the HTL.

As shown above, the possibilities of multifunctional molecules are endless due to their ability to passivate different types of surface defects with multiple functional groups. This opens the door to the engineering of specific molecules with functional groups to combat certain surface defects.

4. Polymers

In addition to small molecules, polymers are utilized by many researchers to passivate the surface defects of PSCs. Polymers often have multiple functional groups, which allows them to passivate multiple defects of perovskite film [76]. Moreover, polymers provide structural integrity, which further enhances the stability of the resulting PSCs compared to small molecules [77,78].

It is common for polymers to have multiple functional groups due to their size. For example, Ma et al. investigated the usage of bis(trifluoromethyl)benzo amide (BTFZA) as a surface passivant of FAMAPb$I_{3-x}Br_x$ perovskite film [79]. Multiple functional groups of BTFZA, such as the amine group, benzene ring, carbonyl group, and trifluoromethyl group, reacted with undercoordinated, positively charged lead ions and passivated the film, which led to an increase in the transport of charged carriers. In addition, BTFZA formed hydrogen bonds with methylammonium and formamidinium groups, which increased the charged carrier extraction and transport. The resulting device, with a structure of glass/ITO/SnO_2/FAMAPb$I_{3-x}Br_x$/BTFZA/Spiro-OMeTAD/Au, had a PCE of 19.85% with an improved fill factor, open-circuit voltage, humidity tolerance, and thermal stability.

One of the main advantages of using polymers as a surface passivant is that, due to their large structure, some polymers have a hydrophobic polytetrafluoroethylene backbone. This enhances the hydrophobicity of the resulting perovskite film, which increases the humidity stability of the PSC. For instance, Shi et al. utilized PEDOT:F, poly(3,4-ethylene dioxythiophene):perfluorinated sulfonic acid ionomers, as a surface passivant of perovskite film [80]. As seen in Figure 11, the PEDOT:F layer between the perovskite layer and HTL not only passivated the undercoordinated Pb^{2+} ions on the perovskite surface with the lone electron pairs on the oxygen atoms of PEDOT but also enhanced the extraction and transport of charged carriers. Furthermore, the perfluorinated sulfonic acid ionomers are hydrophobic due to their polytetrafluoroethylene backbone, which enhances the moisture stability of the PSCs. The resulting device, with a structure of glass/FTO/SnO_2/Cs FAMAPb$I_{3-x}Br_x$/PEDOT:F/Spiro-OMeTAD/Au, had a PCE of 24.81% with enhanced stability.

In some cases, instead of a polytetrafluoroethylene backbone being the cause of the hydrophobicity of the polymer, an extended alkyl chain contributed to the moisture stability of the resulting PSCs. Li et al. utilized butyl-2-(2,3-dimethylpentanamido)-3-methylpentanamide (DPA_4), 2-(2,3-dimethylpentanamido)-*N*-hexyl-3-methyl pentanamide (DPA_6), 2-(2,3-dimethylpentanamido)-3-methyl-*N*-octylpentanamide (DPA_8), and *N*-decyl-2-(2,3-dimethylpentanamido)-3-methylpentanamide (DPA_{10}) as surface passivants of the $MAPbI_3$ perovskite film [81]. These dipeptide molecules were chosen for their carbonyl, ether, and amino groups. The carbonyl and ether groups passivated undercoordinated positively charged lead ions, and the amino group formed hydrogen bonds with iodine ions. Moreover, these dipeptide molecules have extended alkyl chains, which introduces hydrophobic qualities to the perovskite film. The resulting device (glass/ITO/PTAA/$MAPbI_3$/DPA_{10}/PC_{61}BM/BCP/Ag) that was treated with DPA_{10} had a PCE of 20.31% and improved

stability. As seen above, polymers cannot only enhance the moisture stability of the resulting devices by creating a hydrophobic surface but also passivate multiple defects due to their arsenal of multiple functional groups.

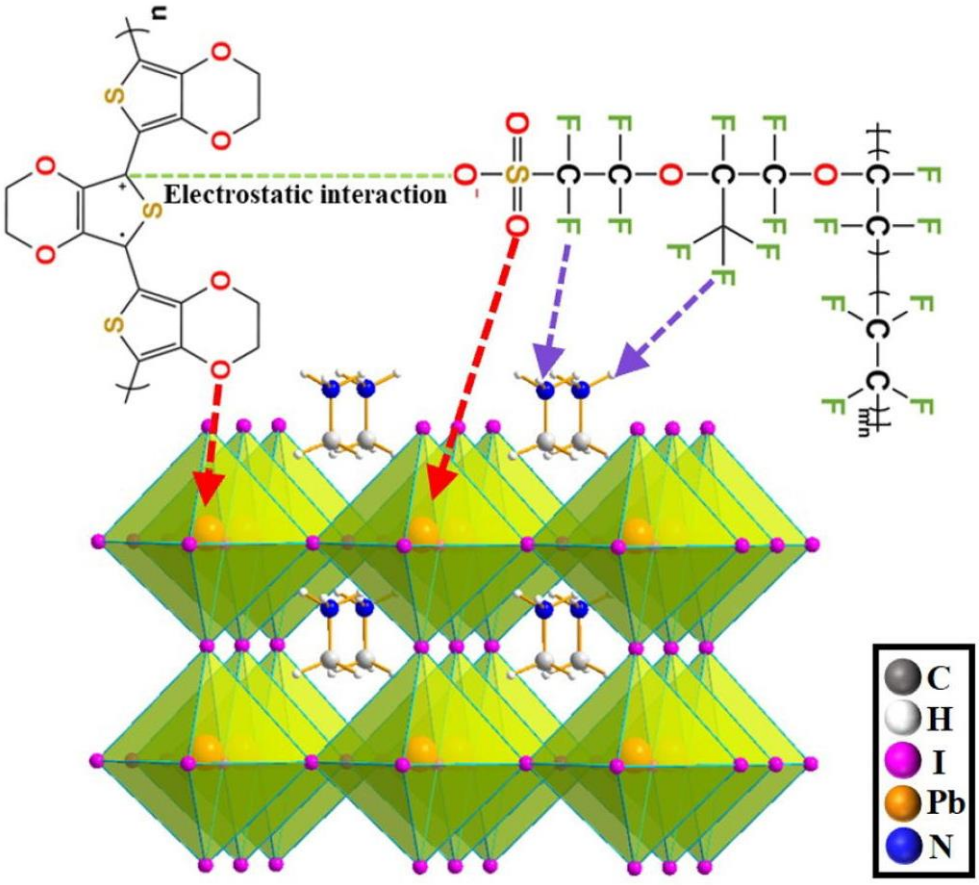

Figure 11. The diagram above illustrates the passivation effect of PEDOT:F on the perovskite surface, as the lone pair of electrons from oxygen atoms are bonding with undercoordinated Pb^{2+} ions [80].

Instead of merely using an existing polymer, some groups resorted to engineering a specific polymer for their needs. For example, Na et al. designed a polymer with a cyano group, $PBDT_2CNBT$, to passivate surface defects and increase the extraction of charge carriers of $FAMAPbI_{3-x}Br_x$-based PSCs [82]. The cyano group can strongly interact with the surface of the perovskite film and passivate surface defects of the perovskite film, in addition to the defects at the grain boundary. The results from X-ray photoelectron spectroscopy demonstrate that the polymer formed a passivation layer on the perovskite film and protected the film from oxidizing when exposed to ambient air. The $PBDT_2CNBT$-treated PSC with a structure of glass/ITO/SnO_2/$FAMAPbI_{3-x}Br_x$/$PBDT_2CNBT$/Spiro-OMeTAD/Au had a PCE of 22.9% and improved light, humidity, and thermal stability.

Similarly, Pu et al. engineered a polymer, a 3D star-shaped polyhedral oligomeric silsesquioxane-poly(trifluoroethylmethacrylate)-b-poly(4-nitro-4′-methacrylate azobenzene) (PTHM), as a surface passivant of $CsFAMAPbI_3$ perovskite film [83]. PTHM is a 3D star-shaped polymer with carboxyl, cyano, and trifluoromethyl groups. When the perovskite film was treated with PTHM, the polymer passivated undercoordinated, positively charged lead ions and prevented ion migrations at the surface and grain boundaries of the perovskite film. The 3D star-shaped structural polymer network enabled this passivant to react better with the 3D perovskite material than the control and enhanced the thermal stability of the resulting device. Additionally, the trifluoromethyl group formed hydrogen bonds with FA^+ and MA^+, which decreased non-radiative recombination and increased the transport of charged carriers. The resulting inverted device with a structure of

glass/NiOx/PTAA/CsFAMAPbI$_3$/PTHM/C$_{60}$-PCBM/BCP/Cr-Au had a PCE of 24.03% with improved operational stability. As shown in the two examples above, engineered polymers are a promising material for surface passivation, as specific structures and functional groups can be chosen specifically for the device. A polymer can be engineered to form a buffer layer on top of the perovskite film and passivate surface defects with the cyano group, while it can also be modified as a 3D star-shaped structural polymer network. The possibility of using an engineered polymer as a surface passivant should be explored in more detail in the future.

In short, polymers have great potential as a surface passivant of PSCs, especially when engineered for specific functional groups and structures to enhance the thermal and environmental stabilities of the resulting PSCs. However, the difference between using a small molecule and a polymer as a surface passivant of PSCs is a field that needs to be further explored in the future.

5. Passivants for Sn-Based PSCs

Sn-based PSCs are utilized for their eco-friendliness and potential usage in tandem solar cells. For example, Sun et al. achieved a certified PCE of 14.3%, establishing one of the highest-performing Sn-based PSCs in the world [84]. However, this device's performance is not comparable to that of its lead-based counterpart, which is due to the differences in the properties of electrons between Sn^{2+} ions and Pb^{2+} ions: Sn^{2+} ions have 5*s* electrons while Pb^{2+} ions have 6*s* electrons [85]. The *5s* electrons of Sn^{2+} ions are more reactive compared to the 6*s* electrons of Pb^{2+} ions. Consequently, Sn-based perovskite, with more defects on the crystal, is susceptible to oxidation reaction, imperfect coverage on the film, and swift crystallization. [86]. The surface of Sn-based perovskite layers is especially weak to oxidation, which causes the weak bond between Sn^{2+} and I^- ions to break, resulting in non-radiative recombination and the degradation of the bulk film [87]. It is worth noting that the Sn-based perovskite layer is more soluble in common solvents, and solvent engineering is required for the passivating layer of perovskite to ensure that the passivation does not negatively affect the perovskite layer. Through solvent engineering, researchers utilize many molecules and polymers to enhance the device performance of Sn-based PSCs.

In order to reduce the negative effects of Sn-based perovskite, which has a more defective crystalline structure than its Pb-based counterpart, Chan et al. utilized iso-butylammonium iodide (*iso*-BAI) to passivate Sn-based PSCs [88]. This group performed solvent engineering to ensure that the solvent used for *iso*-BAI does not dissolve the bulk film. They mixed 2-methyl-2-butanol and chlorobenzene at a ratio of 1:19, respectively, for the *iso*-BAI solution and dynamically spin-coated this solution on the perovskite film, as shown in Figure 12. Although *iso*-BAI is capable of forming a 2D/3D heterostructured perovskite layer, it did not in this case. Instead, the *iso*-BA^+ cations assisted in the recrystallization of the $FASnI_3$ perovskite film by behaving as anchoring sites. These cations acted as a buffer layer to block the perovskite film from making immediate contact with moisture and oxygen, preventing the oxidation reaction and further degradation of the film. This treatment resulted in a better crystallization of the surface than the control, reduced the defects on the surface of the perovskite layer, and enhanced the charge transport. The resulting device with the structure of glass/ITO/PEDOT:PSS/PEAI-$FASnI_3$/*iso*-BAI/BCP/Ag had a PCE of 14.2%, which is higher than the control, at 11.8%.

The usage of a surface passivant for the all-inorganic Cs–Sn–mixed perovskite without lead is explored as well. Zhang et al. utilized 3-thiophenemethylamoonium iodide (3-ThMAI) as a passivant between the $CsSnI_3$ perovskite layer and the ETL [89]. This specific molecule is chosen due to its polarity and electron-rich sulfur atom. Because 3-ThMAI is polar, it induced the formation of a dipole electric field at the interface, which reduced the potential barrier of electron extraction. Furthermore, the sulfur atom interacted with undercoordinated Sn^{2+} ions on the surface of the $CsSnI_3$ perovskite film, which reduced surface defects. The resulting device, with a structure of glass/ITO/PEDOT:PSS/$CsSnI_3$/3-

ThMAI/ICBA/BCP/Ag, had a PCE of 12.05%. This is one of the highest PCEs of $CsSnI_3$-perovskite devices that has been published.

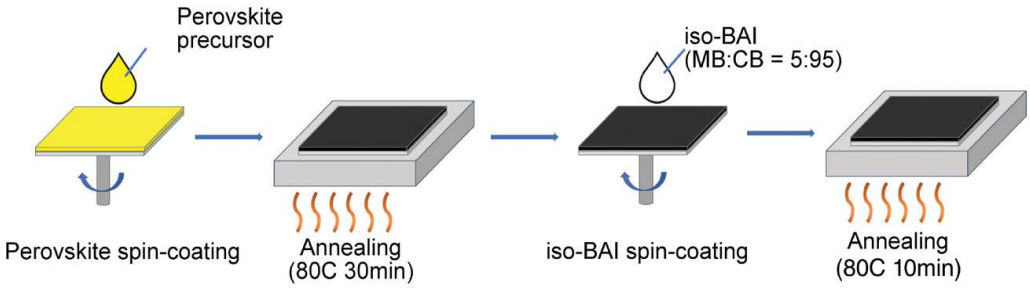

Figure 12. The illustration demonstrates the process of perovskite film and *iso*-BAI treatment [88]. The perovskite precursor solution is spin-coated and annealed at 80 °C for 30 min. Afterward, *iso*-BAI dissolved in 2-methyl-2-butanol and chlorobenzene at a ratio of 5: 95, respectively, is spin-coated on the perovskite film. Lastly, it is annealed at 80 °C for 10 min.

Similarly, Zhang et al. utilized poly-methyl-phenyl-silane (PMPS) as a bifunctional surface passivant of Cs–Sn–mixed PSCs [90]. These specific polysilanes are capable of enhancing both the short-circuit current and the open-circuit voltage by improving the surface morphology of the perovskite film and passivating the undercoordinated Sn^{4+} ions. First, the addition of a PMPS layer to the perovskite film induced an additional growth in the perovskite grains, which resulted in a significant growth in grain size. This PMPS passivation also led to a much smoother surface of the perovskite film and enhanced its crystallinity. Additionally, this molecule is called a bifunctional surface passivant due to its ability to also act as a reducing agent to passivate Sn^{4+} ions on the perovskite film to prevent the oxidation of the perovskite layer. This resulted in reduced trap densities, less non-radiative recombination than before PMPS treatment, enhanced transport of charged carriers, and the improved alignment of energy levels between the perovskite film and the electron transport layer. The resulting device, with a structure of glass/FTO/PEDOT:PSS/$(Cs_{0.02}(FA_{0.9}DEA_{0.1})_{0.98}EDA_{0\cdot01}SnI_3$/PMPS/$C_{60}$/BCP/Ag, had a PCE of 14.18%.

Some groups focused on the use of Sn–Pb–mixed perovskites as a way to transition into the Sn-based PSCs. For instance, Song et al. utilized phenyl-C_{61}-butyric acid methyl ester (PCBM) as a passivant between SnO_2 and the perovskite layer of Sn-Pb-mixed PSCs [91]. This group specifically annealed the PCBM layer at a high temperature of 150 °C to form a thick, hydrophobic PCBM (HT-PCBM) layer on the SnO_2 layer, which resulted in an increase in grain size and reduced the extent to which the SnO_2 layer dissolved when the perovskite precursor or antisolvent were spin-coated. This HT-PCBM treatment facilitated molecular alignment, which enhanced the conductivity of SnO_2 ETL and the charge transport. The reduced trap densities at the SnO_2/perovskite interface from PCBM passivation diminished non-radiative recombination. Furthermore, the hydrophobicity of the HT-PCBM layer prevented the oxidation of SnO_2 and degradation of the perovskite film due to the oxidation of metal oxides. The resulting device, with a structure of glass/ITO/SnO_2/HT-PCBM/$FAMASnPbI_3$/C_{60}/BCP/Al, had a PCE of 15.50% compared to the 6.03% PCE of the control without PCBM passivation. This is one of the highest efficiencies among Sn-Pb-mixed, n-i-p-structured PSCs that has been published.

In short, Sn-based PSCs are an emerging field. A variety of combinations of Sn-based perovskites are being explored by researchers, as shown above: $FASnI_3$, $CsSnI_3$, $(Cs_{0.02}(FA_{0.9}DEA_{0.1})_{0.98}EDA_{0.01}SnI_3$, and $FAMASnPbI_3$. It is expected that more effective passivation schemes for Sn-based perovskites will be developed in further research to take advantage of the eco-friendliness of tin and its applications in tandem solar cells.

6. Conclusions and Outlook

Organic-inorganic perovskite solar cells have achieved significant increases in efficiency and stability in recent years. Because defects on the surface of the perovskite film are the main causes of reduced stability and efficiency, surface passivation is an essential method to further enhance the efficiency and stability of PSCs. Researchers have investigated many different molecules for surface passivation, including molecules that result in an LD/3D perovskite heterostructure, small molecules, and polymers. This review revealed that different passivants have various benefits and hindering effects, and passivants need to be carefully chosen for each perovskite and device structure

According to this review, surface passivation is a promising and cost-effective technique for improving the overall photovoltaic performance of PSCs. Understanding fundamental chemical mechanisms is crucial for effective defect passivation. As a result, researchers can engineer the materials of small molecules or polymers passivating the specific interface of devices made of different perovskite materials and charge transporting layers to optimize the performance of PSCs. The ideal passivants may possess multiple functional groups and be capable of passivating most defects at the perovskite surface and grain boundaries in bulk, creating a buffer layer with a hydrophobic surface to improve environmental stability and inducing favorable energy level alignment for charge transport and collection, improving both efficiency and stability, while such passivants would not induce negative effects, such as increasing resistance and limiting charge transport, or being easily breaking and degrading under increased thermal, moisture and light conditions. Nevertheless, due to the similar mechanisms of operation for PSCs with different types of perovskite than Pb- or Sn-based ones, the findings from this review can be applied to other types of PSCs. Additionally, the observations from this review can be applied to various other perovskite-based optoelectronic devices, such as light-emitting diodes, laser diodes, optical modulators, and optical sensors.

Funding: This work was supported by the National Science Foundation (grant number: ECCS-2053954). This study was also partially supported by the U.S. Department of Energy's Office of Energy Efficiency and Renewable Energy (EERE) under the Solar Energy Technologies Office Award Number DE-EE0010242.

Data Availability Statement: No new data were created or analyzed in this study.

Conflicts of Interest: The authors declare no conflicts of interest.

References

1. Wu, G.; Liang, R.; Ge, M.; Sun, G.; Zhang, Y.; Xing, G. Surface Passivation Using 2D Perovskites toward Efficient and Stable Perovskite Solar Cells. *Adv. Mater.* **2022**, *34*, 2105635. [CrossRef]
2. Akman, E.; Akin, S. Poly(N,N′-bis-4-butylphenyl-N,N′-bisphenyl)benzidine-Based Interfacial Passivation Strategy Promoting Efficiency and Operational Stability of Perovskite Solar Cells in Regular Architecture. *Adv. Mater.* **2020**, *33*, e2006087. [CrossRef] [PubMed]
3. Zhao, B.; Zhang, T.; Liu, W.; Meng, F.; Liu, C.; Chen, N.; Li, Z.; Liu, Z.; Li, X. Recent Progress of Surface Passivation Molecules for Perovskite Solar Cell Applications. *J. Renew. Mater.* **2023**, *11*, 1533–1554. [CrossRef]
4. Zhang, J.; Tang, S.; Zhu, M.; Li, Z.; Cheng, Z.; Xiang, S.; Zhang, Z. The Role of Grain Boundaries in Organic-Inorganic Hybrid Perovskite Solar Cells and Its Current Enhancement Strategies: A Review. *Energy Environ. Mater.* **2024**, *7*, e12696. [CrossRef]
5. Lee, J.-W.; Tan, S.; Han, T.-H.; Wang, R.; Zhang, L.; Park, C.; Yoon, M.; Choi, C.; Xu, M.; Liao, M.E.; et al. Author Correction: Solid-Phase Hetero Epitaxial Growth of α-Phase Formamidinium Perovskite. *Nat. Commun.* **2020**, *11*, 5880. [CrossRef]
6. Kong, J.; Wang, H.; Röhr, J.A.; Fishman, Z.S.; Zhou, Y.; Li, M.; Cotlet, M.; Kim, G.; Karpovich, C.; Antonio, F.; et al. Perovskite Solar Cells with Enhanced Fill Factors Using Polymer-Capped Solvent Annealing. *ACS Appl. Energy Mater.* **2020**, *3*, 7231–7238. [CrossRef]
7. Lee, Y.S.; Do, J.J.; Jung, J.W. A Comparative Study of Surface Passivation of P-i-n Perovskite Solar Cells by Phenethylammonium Iodide and 4-Fluorophenethylammonium Iodide for Efficient and Practical Perovskite Solar Cells with Long-Term Reliability. *J. Alloys Compd.* **2024**, *988*, 174060. [CrossRef]
8. Wang, Y.; Zhao, R.; Yu, X.; Li, L.; Lin, P.; Zhang, S.; Gao, S.; Li, X.; Zhang, W.; Zhang, W.; et al. Surface Passivation of Perovskite by Hole-blocking Layer towards Efficient and Stable Inverted Solar Cells. *Sol. RRL* **2024**, *8*, 2400158. [CrossRef]

9. Dong, P.; Chen, B.; Yao, D.; Li, S.; Su, J.; Zhou, B.; Tian, N.; Zheng, G.; Peng, Y.; Long, F. Comprehensive Interface Engineering Based on Target Anchoring Agents Towards Efficient and Stable Inverted Perovskite Solar Cells. *J. Mater. Chem. A* **2024**, *12*, 6134–6145. [CrossRef]
10. Kim, S.-J.; Cho, I.H.; Nguyen, T.-D.; Hong, Y.-K.; Kim, Y.; Yum, J.-H.; Sivula, K.; Kang, J.; Kim, H.-S.; Zakeeruddin, S.M.; et al. Methylammonium Nitrate-Mediated Crystal Growth and Defect Passivation in Lead Halide Perovskite Solar Cells. *ACS Energy Lett.* **2024**, *9*, 2137–2144. [CrossRef]
11. Yang, Z.; Wei, J.; Zheng, J.; Zhong, Z.; Du, H.; He, Z.; Liu, L.; Ma, Q.; Yu, X.; Wang, Y.; et al. Crystallization Kinetics of Perovskite Films by a Green Mixture Antisolvent for Efficient NIOX-Based Inverted Solar Cells. *ACS Appl. Mater. Interfaces* **2024**, *16*, 19838–19848. [CrossRef] [PubMed]
12. Liu, Y.; Bae, S.; Lee, S.; Wang, A.; Jung, Y.; Lee, D.; Lee, J. Controlled Growth of Uniform and Dense Perovskite Layers on SnO_2 via Interface Passivation by PbS Quantum Dots. *EcoMat* **2024**, *6*, e12456. [CrossRef]
13. Wu, Y.; Zhang, J.; Luo, J.; Wang, M.; Cai, S.; Cai, Q.; Wei, D.; Ji, J.; Zhang, Z.; Li, X. Tailoring Interface and Morphology of TiO_2 Electron Transport Layer with Potassium Bitartrate for High-Performance Perovskite Solar Cells. *Appl. Surf. Sci.* **2024**, *662*, 160139. [CrossRef]
14. Zhou, H.; Sun, Y.; Zhang, M.; Ni, Y.; Zhang, F.; Jeong, S.Y.; Huang, T.; Li, X.; Woo, H.Y.; Zhang, J.; et al. Over 18.2% Efficiency of Layer–by–Layer All–Polymer Solar Cells Enabled by Homoleptic Iridium(III) Carbene Complex as Solid Additive. *Sci. Bull.* **2024**, *69*, 2862–2869. [CrossRef] [PubMed]
15. Tian, H.; Ni, Y.; Zhang, W.; Xu, Y.; Zheng, B.; Jeong, S.Y.; Wu, S.; Ma, Z.; Du, X.; Hao, X.; et al. Over 19.2% Efficiency of Layer-by-Layer Organic Photovoltaics Enabled by a Highly Crystalline Material as an Energy Donor and Nucleating Agent. *Energy Environ. Sci.* **2024**, *17*, 5173–5182. [CrossRef]
16. Chao, L.; Wang, Z.; Xia, Y.; Chen, Y.; Huang, W. Recent Progress on Low Dimensional Perovskite Solar Cells. *J. Energy Chem.* **2018**, *27*, 1091–1100. [CrossRef]
17. Liu, P.; He, X.; Ren, J.; Liao, Q.; Yao, J.; Fu, H. Organic-Inorganic Hybrid Perovskite Nanowire Laser Arrays. *ACS Nano* **2017**, *11*, 5766–5773. [CrossRef]
18. Liu, J.; Xue, Y.; Wang, Z.; Xu, Z.-Q.; Zheng, C.; Weber, B.; Song, J.; Wang, Y.; Lu, Y.; Zhang, Y.; et al. Two-Dimensional $CH_3NH_3PBI_3$ Perovskite: Synthesis and Optoelectronic Application. *ACS Nano* **2016**, *10*, 3536–3542. [CrossRef]
19. Gao, L.; Hu, P.; Liu, S. Low-Dimensional Perovskite Modified 3D Structures for Higher-Performance Solar Cells. *J. Energy Chem.* **2023**, *81*, 389–403. [CrossRef]
20. Yang, Y.; Gao, F.; Gao, S.; Wei, S.-H. Origin of the Stability of Two-Dimensional Perovskites: A First-Principles Study. *J. Mater. Chem. A* **2018**, *6*, 14949–14955. [CrossRef]
21. Ji, T.; Cao, Y.; Lin, D.; Stolar, M.; Berlinguette, C.P. Molecular Interlayer with Large Cations Supports Efficient, Stable Perovskite Solar Cells. *ACS Appl. Energy Mater.* **2024**, *7*, 5371–5378. [CrossRef]
22. Hartono, N.T.P.; Sun, S.; Gélvez-Rueda, M.C.; Pierone, P.J.; Erodici, M.P.; Yoo, J.; Wei, F.; Bawendi, M.; Grozema, F.C.; Sher, M.-J.; et al. The Effect of Structural Dimensionality on Carrier Mobility in Lead-Halide Perovskites. *J. Mater. Chem. A* **2019**, *7*, 23949–23957. [CrossRef]
23. Ge, C.; Xie, L.; Yang, J.; Wei, K.; Wu, T.; Wang, L.; Sun, L.; Zhang, J.; Hua, Y. Holistic Approach to Low-Dimensional Perovskite Enveloping of Internal Interfaces and Grain Boundaries in Perovskite Solar Cells. *Adv. Funct. Mater.* **2024**, *34*, 2313688. [CrossRef]
24. Abate, S.Y.; Jha, S.; Shaik, A.K.; Ma, G.; Emodogo, J.; Pradhan, N.; Gu, X.; Patton, D.; Hammer, N.I.; Dai, Q. Fabrication of 1D/3D Heterostructure Perovskite Layers by Tetrabutylammonium Tetrafluoroborate for High-Performance Devices. *Org. Electron.* **2024**, *125*, 106984. [CrossRef]
25. Zhou, X.; Liang, X.; Wang, F.; Sun, H.; Zhu, Q.; Hu, H. Pyridine Substitution Strategy for One-Dimensional Perovskite: Toward Efficient and Stable Mixed-Dimensional Photovoltaics. *Chem. Eng. J.* **2024**, *493*, 152539. [CrossRef]
26. Cha, J.; Lee, C.B.; Park, S.M.; Baek, D.; Kim, S.; Han, S.G.; Jin, H.; Yang, S.J.; Lim, J.; Kim, K.; et al. Lattice-Matched in-Situ-Formed 1D Perovskite Phase in Multi-Dimensional Solar Cells Achieving High Phase Stability and Favorable Energy Landscape. *Chem. Eng. J.* **2024**, *484*, 149280. [CrossRef]
27. Gu, J.; Sun, X.; Chan, P.F.; Lu, X.; Zeng, P.; Gong, J.; Li, F.; Liu, M. Constructing Low-Dimensional Perovskite Network to Assist Efficient and Stable Perovskite Solar Cells. *J. Energy Chem.* **2024**, *96*, 625–632. [CrossRef]
28. Li, Y.; Duan, Y.; Liu, Z.; Yang, L.; Li, H.; Fan, Q.; Zhou, H.; Sun, Y.; Wu, M.; Ren, X.; et al. In-Situ-Synthesized Low-Dimensional Perovskite for >25% Efficiency Stable MA-Free Perovskite Solar Cells. *Adv. Mater.* **2024**, *36*, e2310711. [CrossRef]
29. Su, J.; Hu, T.; Chen, X.; Zhang, X.; Fang, N.; Hao, J.; Guo, H.; Jiang, S.; Gu, D.; Qiu, J.; et al. Multi-Functional Interface Passivation via Guanidinium Iodide Enables Efficient Perovskite Solar Cells. *Adv. Funct. Mater.* **2024**, 2406324. [CrossRef]
30. Jeong, J.; Kim, M.; Seo, J.; Lu, H.; Ahlawat, P.; Mishra, A.; Yang, Y.; Hope, M.A.; Eickemeyer, F.T.; Kim, M.; et al. Pseudo-Halide Anion Engineering for α-$FAPbI_3$ Perovskite Solar Cells. *Nature* **2021**, *592*, 381–385. [CrossRef]
31. Wang, Z.; Ma, T.; Wang, J.; Zhu, S.; Zhang, M.; Guo, M. Surface Passivation for Efficient and Stable Perovskite Solar Cells in Ambient Air: The Structural Effect of Amine Molecules. *Ceram. Int.* **2024**, *50*, 7528–7537. [CrossRef]
32. Choi, E.; Lee, J.; Anaya, M.; Mirabelli, A.; Shim, H.; Strzalka, J.; Lim, J.; Yun, S.; Dubajic, M.; Lim, J.; et al. Synergetic Effect of Aluminum Oxide and Organic Halide Salts on Two-Dimensional Perovskite Layer Formation and Stability Enhancement of Perovskite Solar Cells. *Adv. Energy Mater.* **2023**, *13*, 2301717. [CrossRef]

33. Luo, Y.; Liu, K.; Yang, L.; Feng, W.; Zheng, L.; Shen, L.; Jin, Y.; Fang, Z.; Song, P.; Tian, W.; et al. Dissolved-Cl_2 Triggered Redox Reaction Enables High-Performance Perovskite Solar Cells. *Nat. Commun.* **2023**, *14*, 3738. [CrossRef] [PubMed]
34. Yoo, J.J.; Seo, G.; Chua, M.R.; Park, T.G.; Lu, Y.; Rotermund, F.; Kim, Y.-K.; Moon, C.S.; Jeon, N.J.; Correa-Baena, J.-P.; et al. Efficient Perovskite Solar Cells via Improved Carrier Management. *Nature* **2021**, *590*, 587–593. [CrossRef]
35. Tan, L.; Shen, L.; Song, P.; Luo, Y.; Zheng, L.; Tian, C.; Xie, L.; Yang, J.; Wei, Z. Pure Chloride 2D/3D Heterostructure Passivation for Efficient and Stable Perovskite Solar Cells. *Adv. Energy Sustain. Res.* **2023**, *4*. [CrossRef]
36. Li, Z.; Sun, A.; Zheng, Y.; Zhuang, R.; Wu, X.; Tian, C.; Tang, C.; Liu, Y.; Ouyang, B.; Du, J.; et al. Efficient Charge Transport in Inverted Perovskite Solar Cells via 2D/3D Ferroelectric Heterojunction. *Small Methods* **2024**, 2400425. [CrossRef]
37. Gong, H.; Song, Q.; Zhu, T.; Zhang, C.; Huang, X.; Jing, X.; You, F.; Liang, C.; He, Z. Forming Enlarged Grain and Fixed Boundary via a Two-Step Surface Modification to Achieve Stable Inverted Perovskite Solar Cells. *Chem. Eng. J.* **2024**, *483*, 149382. [CrossRef]
38. Metrangolo, P.; Canil, L.; Abate, A.; Terraneo, G.; Cavallo, G. Halogen Bonding in Perovskite Solar Cells: A New Tool for Improving Solar Energy Conversion. *Angew. Chem. Int. Ed.* **2022**, *61*, e202114793. [CrossRef]
39. Sun, Q.; Meng, X.; Liu, G.; Duan, S.; Hu, D.; Shen, B.; Kang, B.; Silva, S.R.P. SNO_2 Surface Modification and Perovskite Buried Interface Passivation by 2,5-Furandicarboxylic Acid for Flexible Perovskite Solar Cells. *Adv. Funct. Mater.* **2024**, 2404686. [CrossRef]
40. Shao, W.; Wang, H.; Fu, S.; Ge, Y.; Guan, H.; Wang, C.; Wang, C.; Wang, T.; Ke, W.; Fang, G. Tailoring Perovskite Surface Potential and Chelation Advances Efficient Solar Cells. *Adv. Mater.* **2024**, *36*, e2310080. [CrossRef]
41. Chen, Z.; Jiang, S.; Liu, Z.; Li, Y.; Shi, J.; Wu, H.; Luo, Y.; Li, D.; Meng, Q. Interfacial Defect Passivation via Imidazolium Bromide for Efficient, Stable Perovskite Solar Cells. *J. Mater. Chem. A* **2024**, *12*, 16070–16078. [CrossRef]
42. Liu, Z.; Shao, L.; Zeng, F.; Bian, S.; Liu, B.; Wang, Y.; Wu, Y.; Shao, Y.; Zhang, H.; Zhang, Y.; et al. Dual Modification Engineering Enabled Efficient Perovskite Solar Cells with High Open-Voltage of 1.233 V. *Chem. Eng. J.* **2024**, *488*, 151077. [CrossRef]
43. Wang, W.-T.; Chiang, C.-H.; Zhang, Q.; Mu, Y.; Wu, C.-G.; Feng, S.-P. Defect-Induced Dipole Moment Change of Passivators for Improving the Performance of Perovskite Photovoltaics. *ACS Energy Lett.* **2024**, *9*, 2982–2989. [CrossRef]
44. Yang, B.; Cai, B.; Zhou, T.; Zheng, X.; Zhang, W.-H. Facile and Sustainable Interface Modulation via a Self-Assembly Phosphonate Molecule for Efficient and Stable Perovskite Photovoltaics. *Chem. Eng. J.* **2024**, *488*, 150861. [CrossRef]
45. Xu, Y.; Zhang, H.; Liu, F.; Li, R.; Jing, Y.; Wang, X.; Wu, J.; Zhang, J.; Lan, Z. 2-Iodoaniline-Modified High-Efficiency Carbon-Based CsPbIBr2 Perovskite Solar Cells. *Appl. Surf. Sci.* **2024**, *658*, 159831. [CrossRef]
46. Kim, H.; Choi, K.; Yoon, G.W.; Kim, D.; Lee, D.H.; Choi, Y.; Jung, H.S.; Song, S.; Park, T. Modulating Molecular Interaction of Zwitterion toward Rational Interface Engineering of Perovskite Solar Cells. *Adv. Energy Mater.* **2024**, *14*, 2401263. [CrossRef]
47. Cheng, C.; Yao, Y.; Li, L.; Zhao, Q.; Zhang, C.; Zhong, X.; Zhang, Q.; Gao, Y.; Wang, K. A Novel Organic Phosphonate Additive Induced Stable and Efficient Perovskite Solar Cells with Efficiency over 24% Enabled by Synergetic Crystallization Promotion and Defect Passivation. *Nano Lett.* **2023**, *23*, 8850–8859. [CrossRef]
48. He, Q.; Zhang, Z.; Chen, A.; Zhang, T.; Chen, X.; Bian, X.; Xu, G.; Chen, T.; Pan, S.; Yu, J.; et al. Surface Passivation with an Electron-Donating Sulfonate Group for High-Performance and Stable Perovskite Solar Cells. *J. Mater. Chem. A* **2024**, *12*, 12545–12551. [CrossRef]
49. Yuan, X.; Ling, X.; Wang, H.; Shen, C.; Li, R.; Deng, Y.; Chen, S. Modulation on Electrostatic Potential to Build a Firm Bridge at NiO /Perovskite Interface for Efficient and Stable Perovskite Solar Cells. *J. Energy Chem.* **2024**, *96*, 249–258. [CrossRef]
50. Wang, X.; Jiang, J.; Liu, Z.; Li, A.; Miyasaka, T.; Wang, X. Zwitterion Dual-Modification Strategy for High-Quality NIO_X and Perovskite Films for Solar Cells. *Small* **2024**, *20*, e2400356. [CrossRef]
51. Yu, T.; Ma, Z.; Huang, Z.; Li, Y.; Tan, J.; Li, G.; Hou, S.; Du, Z.; Liu, Z.; Li, Y.; et al. Amino Pyridine Iodine as an Additive for Defect-Passivated Perovskite Solar Cells. *ACS Appl. Mater. Interfaces* **2023**, *15*, 55813–55821. [CrossRef] [PubMed]
52. Hong, S.; Cui, A.; Liu, S.; Yang, S. Guanidine Carbonate Modified TIO_2/Perovskite Interface for Efficient and Stable Planar Perovskite Solar Cells. *Org. Electron.* **2024**, *130*, 107063. [CrossRef]
53. Wu, C.; Wang, R.; Lin, Z.; Yang, N.; Wu, Y.; Ouyang, X. Simultaneous Dual-Interfaces Modification Based on Mixed Cations for Efficient Inverted Perovskite Solar Cells with Excellent Stability. *Chem. Eng. J.* **2024**, *493*, 152899. [CrossRef]
54. Liu, C.; Shi, P.; Li, C.; Huang, W.; Yang, X.; Yavuz, I.; Xue, J.; Liu, R.; Wang, R. Manipulating the Interfacial Dipole toward High-Performance Perovskite Solar Cells via Conjugated Organic Ammonium. *ACS Sustain. Chem. Eng.* **2024**, *12*, 8923–8929. [CrossRef]
55. Jeong, J.; Chawanpunyawat, T.; Kim, M.; Sláma, V.; Lempesis, N.; Agosta, L.; Carnevali, V.; Zhang, Q.; Eickemeyer, F.T.; Pfeifer, L.; et al. Carbazole Treated Waterproof Perovskite Films with Improved Solar Cell Performance. *Adv. Energy Mater.* **2024**, 2401965. [CrossRef]
56. Jiang, Q.; Zhao, Y.; Zhang, X.; Yang, X.; Chen, Y.; Chu, Z.; Ye, Q.; Li, X.; Yin, Z.; You, J. Surface Passivation of Perovskite Film for Efficient Solar Cells. *Nat. Photonics* **2019**, *13*, 460–466. [CrossRef]
57. Ma, Y.; Li, F.; Gong, J.; Wang, L.; Tang, X.; Zeng, P.; Chan, P.F.; Zhu, W.; Zhang, C.; Liu, M. Bi-Molecular Kinetic Competition for Surface Passivation in High-Performance Perovskite Solar Cells. *Energy Environ. Sci.* **2024**, *17*, 1570–1579. [CrossRef]
58. Shi, Z.; Guo, R.; Luo, R.; Wang, X.; Ma, J.; Feng, J.; Niu, X.; Alvianto, E.; Jia, Z.; Guo, X.; et al. "T-Shaped" Carbazole Alkylammonium Cation Passivation in Perovskite Solar Cells. *ACS Energy Lett.* **2024**, *9*, 419–427. [CrossRef]
59. Wang, J.; Wu, Y.; Zhao, J.; Lu, S.; Lu, J.; Sun, J.; Wu, S.; Zheng, X.; Zheng, X.; Tang, X.; et al. Unraveling the Molecular Size Effect on Surface Engineering of Perovskite Solar Cells. *Small Methods* **2024**, 2400043. [CrossRef]

60. Yang, P.; Wu, J.; Yang, J.; Ke, C.; Lin, W.; Huang, Y.; Tian, J.; Wang, Y.; Sun, W.; Lan, Z.; et al. Effective Passivation of Defects in High-Performance Tin Oxide-Based Perovskite Solar Cells Using Guanidinium Phosphate Additives. *Surf. Interfaces* **2024**, *44*, 103700. [CrossRef]
61. Zhang, J.; Zheng, X.; Cui, Q.; Yao, Y.; Su, H.; She, Y.; Zhu, Y.; Li, D.; Liu, S. Manipulating the Crystallization of Perovskite via Metal-Free DABCO-NH_4CL_3 Addition for High Efficiency Solar Cells. *Adv. Funct. Mater.* **2024**, *34*, 2400043. [CrossRef]
62. Yang, Z.; Chen, J.; Li, M.; Qi, M.; Zhang, G.; Chen, R.; Hu, J.; Liu, X.; Qin, C.; Xiao, L.; et al. 4-Methoxy Phenethylammonium Halide Salts for Surface Passivation of Perovskite Films towards Efficient and Stable Solar Cells. *Chem. Eng. J.* **2024**, *494*, 152955. [CrossRef]
63. Wang, Y.; Wang, F.; Song, J.; Ye, J.; Cao, J.; Yin, X.; Su, Z.; Jin, Y.; Hu, L.; Zuilhof, H.; et al. Ethyl Thioglycolate Assisted Multifunctional Surface Modulation for Efficient and Stable Inverted Perovskite Solar Cells. *Adv. Funct. Mater.* **2024**, *34*, 2402632. [CrossRef]
64. Guo, T.; Liang, Z.; Liu, B.; Huang, Z.; Xu, H.; Tao, Y.; Zhang, H.; Zheng, H.; Ye, J.; Pan, X. Designing Surface Passivators through Intramolecular Potential Manipulation for Efficient and Stable Perovskite Solar Cells. *Small* **2024**, *20*, 2402197. [CrossRef]
65. Liu, W.; Zhang, S.; Kong, F.; Shen, Z.; Chen, C.; Pan, X.; Zhao, C.; Zhang, J.; Ghadari, R.; Bao, M.; et al. Synergistic Resonant Molecular Passivator of Various Defects for High-Performance Perovskite Solar Cells. *Mater. Today Energy* **2024**, *40*, 101511. [CrossRef]
66. Qi, D.; Cao, Y.; Feng, X.; Ge, J.; Yan, N.; Yuan, Y.; Zhang, J.; Song, F.; Wang, K.; Liu, S.; et al. Implementation of a Multi-Functional-Group Strategy for Enhanced Performance of Perovskite Solar Cells through the Incorporation of 3-Amino-4-Phenylbutyric Acid Hydrochloride. *Small* **2024**, *20*, e2401487. [CrossRef]
67. Kim, Y.; Lee, H.; Lee, C.; Kim, B.; Kwon, N.; Son, T.; Lee, J.; Sin, J.; Shin, T.; Yang, J.; et al. Enhancing Performance of Two-step Fabricated Perovskite Solar Cells with Sulfonium Triflate-based Additive. *EcoMat* **2024**, *6*, e12446. [CrossRef]
68. Gu, S.; He, J.; Wang, S.; Li, D.; Liu, H.; Li, X. In-Situ Reaction Modification of Isocyanate Derivatives with Hole-Transport Units on Perovskite Film Surface for Efficient and Stable Solar Cells. *Nano Energy* **2024**, *127*, 109715. [CrossRef]
69. Wang, Z.; Wang, J.; Zhu, S.; Ma, T.; Zhang, M.; Guo, M. Hydrogen Bond Network for Efficient and Stable Fully Ambient Air-Processed Perovskite Solar Cells with Over 21% Efficiency. *ACS Sustain. Chem. Eng.* **2023**, *11*, 14559–14571. [CrossRef]
70. Liu, J.; Chen, J.; Xie, L.; Yang, S.; Meng, Y.; Li, M.; Xiao, C.; Zhu, J.; Do, H.; Zhang, J.; et al. Alkyl Chains Tune Molecular Orientations to Enable Dual Passivation in Inverted Perovskite Solar Cells. *Angew. Chem. Int. Ed.* **2024**, *63*, e202403610. [CrossRef]
71. Zhu, H.; Liu, Y.; Eickemeyer, F.T.; Pan, L.; Ren, D.; Ruiz-Preciado, M.A.; Carlsen, B.; Yang, B.; Dong, X.; Wang, Z.; et al. Tailored Amphiphilic Molecular Mitigators for Stable Perovskite Solar Cells with 23.5% Efficiency. *Adv. Mater.* **2020**, *32*, e1907757. [CrossRef]
72. Wu, Y.; Lu, C.; Gao, F.; Li, Y.; Shi, B.; Cai, X.; Yang, F.; Zhang, J.; Liu, S. 2-Amino-5-Chlorobenzophenone Passivating Perovskite Films Using Multiple Functional Groups towards High-Performance Solar Cells. *J. Mater. Chem. C* **2023**, *11*, 4393–4403. [CrossRef]
73. Lu, C.; Wu, Y.; Gao, F.; Li, Y.; Shi, B.; Cai, X.; Zhang, J.; Yang, F.; Liu, S.F. 3-Ethoxy-4-Hydroxybenzadehyde Surface Passivation of Perovskite Films Enables Exceeding 24% Efficiency in Solar Cells. *ACS Appl. Energy Mater.* **2023**, *6*, 6981–6992. [CrossRef]
74. Zhang, S.; Tian, T.; Li, J.; Su, Z.; Jin, C.; Su, J.; Li, W.; Yuan, Y.; Tong, J.; Peng, Y.; et al. Surface Passivation with Tailoring Organic Potassium Salt for Efficient $FAPbI_3$ Perovskite Solar Cells and Modules. *Adv. Funct. Mater.* **2024**, *34*, 2401945. [CrossRef]
75. Bian, S.; Wang, Y.; Zeng, F.; Liu, Z.; Liu, B.; Wu, Y.; Shao, L.; Shao, Y.; Zhang, H.; Liu, S.; et al. Multifunctional Interfacial Molecular Bridge Enabled by an Aggregation-Induced Emission Strategy for Enhancing Efficiency and UV Stability of Perovskite Solar Cells. *J. Energy Chem.* **2024**, *95*, 588–595. [CrossRef]
76. Zuo, L.; Guo, H.; deQuilettes, D.W.; Jariwala, S.; De Marco, N.; Dong, S.; DeBlock, R.; Ginger, D.S.; Dunn, B.; Wang, M.; et al. Polymer-Modified Halide Perovskite Films for Efficient and Stable Planar Heterojunction Solar Cells. *Sci. Adv.* **2017**, *3*, e1700106. [CrossRef]
77. Jia, S.; Yang, J.; Wang, T.; Pu, X.; Chen, H.; He, X.; Feng, G.; Chen, X.; Bai, Y.; Cao, Q.; et al. In Situ Polymerization of Water-induced 1,3-phenylene Diisocyanate for Enhanced Efficiency and Stability of Inverted Perovskite Solar Cells. *Interdiscip. Mater.* **2024**, *3*, 316–325. [CrossRef]
78. Wang, Y.; Cheng, Y.; Yin, C.; Zhang, J.; You, J.; Wang, J.; Wang, J.; Zhang, J. Manipulating Crystal Growth and Secondary Phase PbI_2 to Enable Efficient and Stable Perovskite Solar Cells with Natural Additives. *Nano-Micro Lett.* **2024**, *16*, 183. [CrossRef]
79. Ma, C.; Zhang, C.; Chen, S.; Ye, Y.; Sun, L.; Gao, L.; Sulaiman, Y.; Ma, T.; Chen, M. Interfacial Defect Passivation by Multiple-Effect Molecule for Efficient and Stable Perovskite Solar Cells. *Sol. Energy Mater. Sol. Cells* **2023**, *262*, 112499. [CrossRef]
80. Shi, C.; Li, J.; Xiao, S.; Wang, Z.; Xiang, W.; Wu, R.; Liu, Y.; Zhou, Y.; Ke, W.; Fang, G.; et al. Alcohol-Dispersed Polymer Complex as an Effective and Durable Interface Modifier for n-i-p Perovskite Solar Cells. *J. Energy Chem.* **2024**, *93*, 243–252. [CrossRef]
81. Li, M.; Yue, Z.; Ye, Z.; Li, H.; Luo, H.; Yang, Q.; Zhou, Y.; Huo, Y.; Cheng, Y. Improving the Efficiency and Stability of $MAPBI_3$ Perovskite Solar Cells by Dipeptide Molecules. *Small* **2024**, *20*, e2311400. [CrossRef] [PubMed]
82. Na, H.; Li, M.Q.; Cha, J.; Kim, S.; Jin, H.; Baek, D.; Kim, M.K.; Sim, S.; Lee, M.; Kim, M.; et al. Passivating Detrimental Grain Boundaries in Perovskite Films with Strongly Interacting Polymer for Achieving High-Efficiency and Stable Perovskite Solar Cells. *Appl. Surf. Sci.* **2023**, *626*, 157209. [CrossRef]
83. Pu, X.; Zhao, J.; Li, Y.; Zhang, Y.; Loi, H.-L.; Wang, T.; Chen, H.; He, X.; Yang, J.; Ma, X.; et al. Stable NiOx-Based Inverted Perovskite Solar Cells Achieved by Passivation of Multifunctional Star Polymer. *Nano Energy* **2023**, *112*, 108506. [CrossRef]

84. Sun, C.; Yang, P.; Nan, Z.; Tian, C.; Cai, Y.; Chen, J.; Qi, F.; Tian, H.; Xie, L.; Meng, L.; et al. Well-Defined Fullerene Bisadducts Enable High-Performance Tin-Based Perovskite Solar Cells. *Adv. Mater.* **2023**, *35*, e2205603. [CrossRef] [PubMed]
85. Xiao, Z.; Song, Z.; Yan, Y. From Lead Halide Perovskites to Lead-Free Metal Halide Perovskites and Perovskite Derivatives. *Adv. Mater.* **2019**, *31*, e1803792. [CrossRef]
86. Cao, J.; Liu, C.; Xu, Y.; Loi, H.; Wang, T.; Li, M.G.; Liu, L.; Yan, F. High-Performance Ideal Bandgap SN-PB Mixed Perovskite Solar Cells Achieved by MXENE Passivation. *Small* **2024**, 2403920. [CrossRef]
87. Ricciarelli, D.; Meggiolaro, D.; Ambrosio, F.; De Angelis, F. Instability of Tin Iodide Perovskites: Bulk p-Doping versus Surface Tin Oxidation. *ACS Energy Lett.* **2020**, *5*, 2787–2795. [CrossRef]
88. Chan, P.F.; Qin, M.; Su, C.; Ye, L.; Wang, X.; Wang, Y.; Guan, X.; Lu, Z.; Li, G.; Ngai, T.; et al. ISO-BAI Guided Surface Recrystallization for over 14% Tin Halide Perovskite Solar Cells. *Adv. Sci.* **2024**, *11*, e2309668. [CrossRef]
89. Zhang, Z.; Yu, H.; Huang, J.; Liu, Z.; Sun, Q.; Li, X.; Dai, L.; Shen, Y.; Wang, M. Over 12% Efficient CsSnI3 Perovskite Solar Cells Enabled by Surface Post-Treatment with Bi-Functional Polar Molecules. *Chem. Eng. J.* **2024**, *490*, 151561. [CrossRef]
90. Zhang, Z.; Liu, J.; Bi, H.; Wang, L.; Shen, Q.; Hayase, S. Over 14% Efficiency of Highly Reproducible Sn Perovskite Solar Cell via Defect Passivation and Morphology Repairment. *Chem. Eng. J.* **2024**, *483*, 149345. [CrossRef]
91. Song, T.; Jang, H.; Seo, J.; Roe, J.; Song, S.; Kim, J.W.; Yeop, J.; Lee, Y.; Lee, H.; Cho, S.; et al. Enhancing Performance and Stability of Sn–Pb Perovskite Solar Cells with Oriented Phenyl-C_{61}-Butyric Acid Methyl Ester Layer via High-Temperature Annealing. *ACS Nano* **2024**, *18*, 2992–3001. [CrossRef] [PubMed]